NGR-14-005-181

AERONOMY REPORT
NO. 83

A ROCKET-BORNE PULSE-HEIGHT ANALYZER FOR ENERGETIC PARTICLE MEASUREMENTS

by
W. Leung
L. G. Smith
H. D. Voss

March 1, 1979

Aeronomy Laboratory
Department of Electrical Engineering
University of Illinois
Urbana, Illinois

CITATION POLICY

A E R O N O M Y   R E P O R T

N O.   83
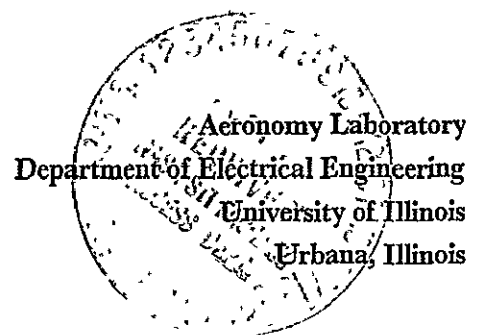
A ROCKET-BORNE PULSE-HEIGHT ANALYZER

FOR ENERGETIC PARTICLE MEASUREMENTS

by

W. Leung
L. G. Smith
H. D. Voss

March 1, 1979

Aeronomy Laboratory
Department of Electrical Engineering
University of Illinois
Urbana, Illinois

ABSTRACT

The development of a rocket-borne pulse-height analyzer (PHA) for the measurement of energetic particles is described. The PHA basically resembles a time-sharing multiplexing data-acquisition system which acquires analog data (from energetic particle spectrometers) and converts them into digital code.

The PHA simultaneously acquires pulse-height information from the analog signals of the four input channels and sequentially multiplexes the digitized data to a microprocessor. The PHA also features a sample-and-hold output where analog data from the four input channels are sampled sequentially and sent to the ground station through a telemetry (TM) channel.

The PHA together with the microprocessor form an on-board real-time data-manipulation system. The system processes data obtained during the rocket flight and reduces the amount of data to be sent back to the ground station. Consequently the data-reduction process for the rocket experiments is speeded up.

By using a time-sharing technique, the throughput rate of the microprocessor is increased. Moreover, data from several particle spectrometers are manipulated to share one information channel; consequently, the TM capacity is increased.

The output of the S/H is analog and, therefore, has a very high amplitude resolution. The output of the microprocessor has sixteen levels of quantization which still offers an output resolution higher than that of the data-manipulation system previously used.

TABLE OF CONTENTS

LIST OF TABLES

LIST OF FIGURES

1. INTRODUCTION

This report is a part of a joint U.S./U.S.S.R. investigation of the nighttime E-region ionization sources in the atmosphere in the vicinity of Wallops Island, Virginia. The main purpose of this investigation was to resolve the controversial results of previous experiments regarding the evidence for energetic particles as a source of ionization in the nighttime E region.

The program included the launch of nine sounding rockets: Five MR-12 from the U.S.S.R. were to have been launched from the Soviet research ship, Professor Vize, off the coast of Wallops Island and four from the U.S.A. were to have been launched from the NASA rocket base on Wallops Island. The four U.S. sounding rockets comprise one Nike Tomahawk and three Nike Apaches. The two identical pulse-height analyzers (PHA) described in this report are data-acquisition systems included in the payloads of the two Nike Apache rockets, 14.542 and 14.543, prepared at the University of Illinois.

The PHA together with the on-board Z-80 microprocessor comprise a rocket-borne data-manipulation system. The system manipulates the input data from the energetic particle detectors so as to reduce the large amount of data to be sent back to the ground station and, therefore, it simplifies the data reduction process of the rocket experiments.

The evidence for ionization sources in the nighttime E region is briefly discussed in Chapter 2. The nature of the ionization sources is then considered. The investigation of energetic particles as the nighttime ionization source is introduced as the main objective of this rocket experiment.

The concept of the data-acquisition system is described in Chapter 3 as it sets the basic design scheme of the PHA. The function of the system, its design alternatives and performance factors such as noise immunity and output error are also discussed.

The design constraints and the general description of the PHA are presented in Chapter 4. The input system is introduced. The basic functions and equivalent circuit models of its components (including six solid-state detectors, an electrostatic analyzer, a magnetometer, six preamplifiers and four shaping circuits) are also briefly discussed.

Chapter 5 describes in detail the design of the PHA. The electronic circuits of individual building blocks of the PHA are explained. The interfaces between the building blocks are described and the input-output factors are discussed. The data-processing error introduced by each stage is analyzed.

Chapter 6 describes some results obtained from the launch of Nike Apache 14.543. Suggestions for additional data reduction are also discussed.

The conclusion of the experiment and suggestions for future work are given in Chapter 7. Since the design of the PHA was completed, integration technology has enabled the manufacture of the whole data-acquisition system in one integrated circuit. The utilization of a particular IC in the design of the PHA is described. In addition, a new design which utilizes small-size voltage-to-frequency converters to replace the A/D converter in the conventional data-acquisition system is discussed.

2. THE *E* REGION AT NIGHT

The difference between daytime and nighttime electron-density profiles in the altitude range between 50 to 190 km are illustrated in Figure 2.1. The profiles are the results of two rocket experiments, on 10 August 1973 and 29 June 1974, respectively, at Wallops Island. The ionization of the atmosphere in the *E* region during the day is due mainly to solar radiation. After sunset the ionization rate decreases considerably. The ionization rate at night is not zero; in subsequent sections the magnitude of the ionization rate will be established and the nature of the source considered.

2.1 *Evidence for Ionization Sources in the Nighttime* E *Region*

Sources of ionization must be present in the *E* region in order to sustain the nighttime ionization, especially for the intermediate layer between 110 to 180 km. In the absence of ionization sources the nighttime ionization, as a remnant part of the daytime ionization, is determined by the recombination rate of the electrons with NO^+ and O_2^+. The mathematical model described by the equation of continuity, in the absence of ionization sources yields an electron-density profile different from the one shown in Figure 2.1 [see *Voss and Smith,* 1979].

Figure 2.2 compares the results of three nighttime rocket experiments. The electron-density profiles are found to vary with magnetic activity. Average ionization rates in the intermediate layer (110 to 180 km) are calculated by using data obtained in different rocket experiments under different magnetic conditions characterized by the three-hour planetary index Kp [see *Voss and Smith,* 1977]. The ionization rates are found to have a strong correlation with the magnetic activity. The variation of ionization with the magnetic activity suggests the importance of energetic particles as an ionization source in the nighttime *E* region.

The existence of ionization sources is confirmed by other experiments. Results obtained from several rocket experiments performed by different scientific groups in different places of the earth clearly show the existence of energetic particles in the nighttime *E* region. Examples of these experiments and their results can be found in *Hill et al.* [1970], *Hayakawa et al.* [1973], and *Voss and Smith* [1974, 1977].

2.2 *Sources of Ionization in the Nighttime* E *Region*

2.2.1 *Ionization due to ultraviolet radiation.* Ultraviolet radiation at night from the geocorona and extraterrestrial origin can excite and ionize the
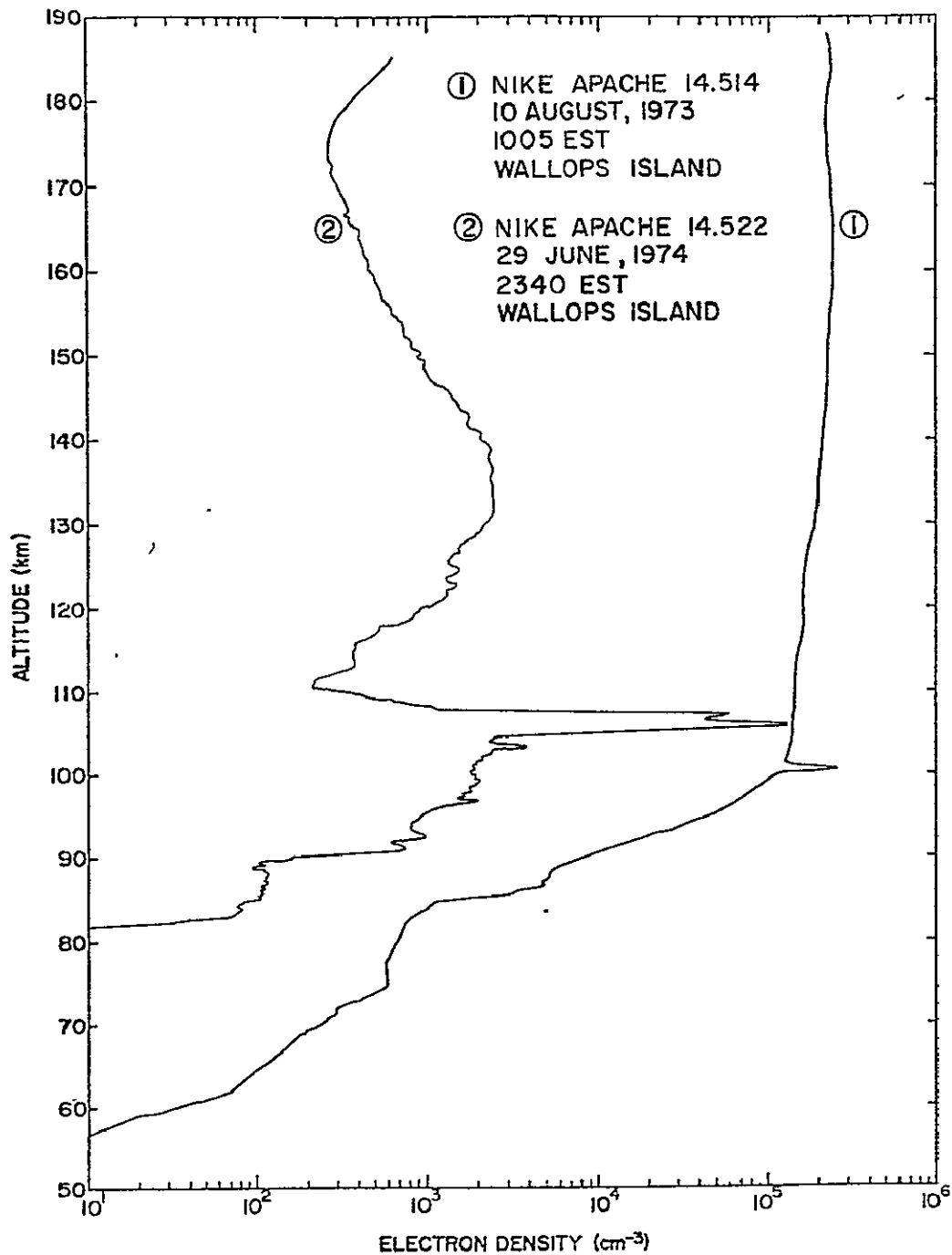
Figure 2.1 Profile 1 is representative of the daytime electron density
$(10^5$ cm$^{-3})$. Towards night this electron density rapidly
decays to a lower nighttime equilibrium level of 10^3 cm^{-3}
(Profile 2). The nighttime density profile shows much
variability and structure [*Voss and Smith*, 1977].
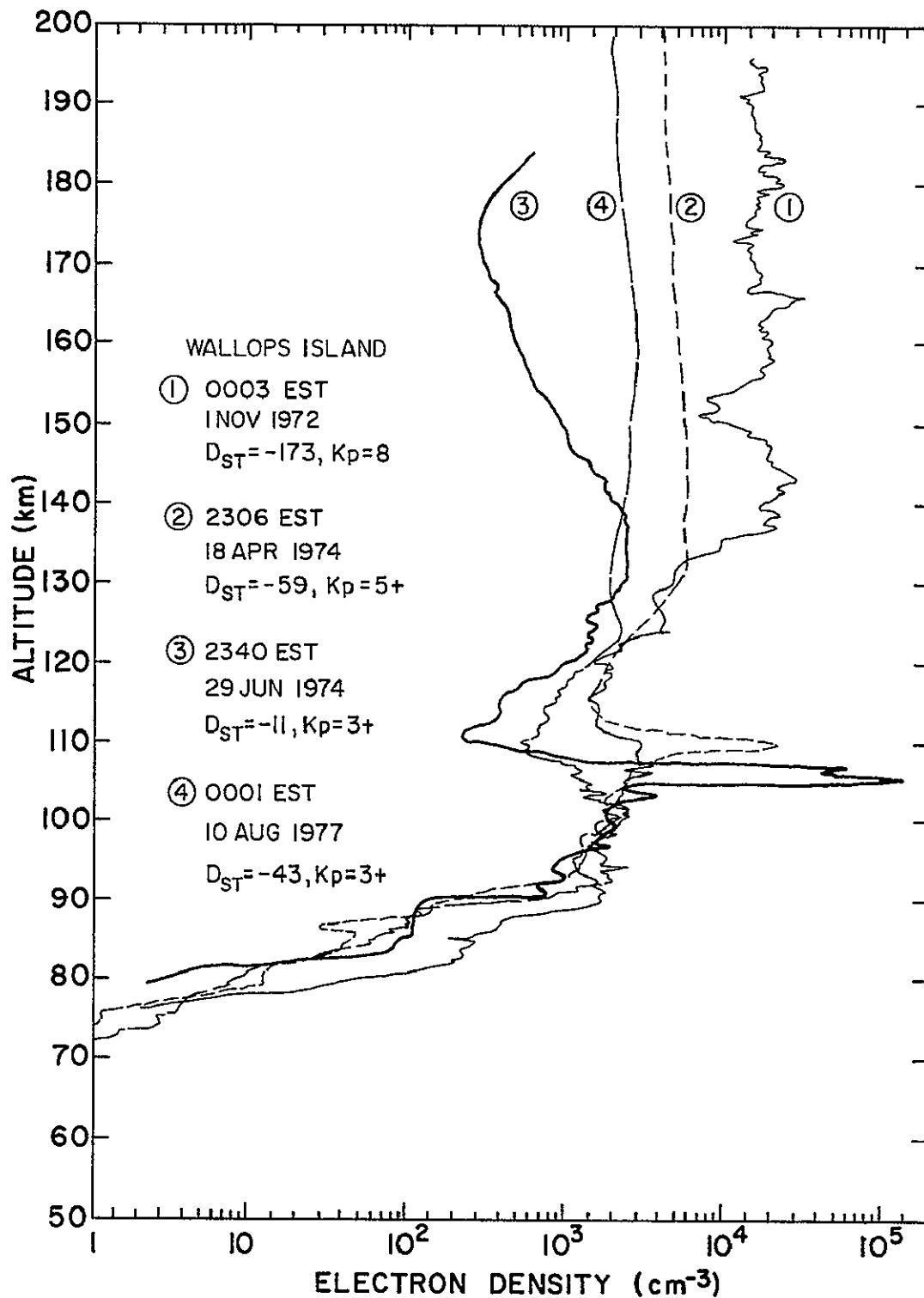
Figure 2.2 Four electron density profiles at Wallops Island near
midnight during various disturbed conditions. The
magnetic index $I \equiv Kp + \ln|D_{ST}|$ is 13.2, 9.4, 5.7,
and 7.1 for profiles 1, 2, 3, and 4, respectively.

atmospheric constituents in the region above 80 km. The hydrogen and helium atoms in the outer atmosphere of the earth (geocorona) absorb energy from solar radiation. These excited atoms release their energy in the form of reradiation at certain frequencies. Part of the radiation scatters into the nighttime ionosphere and becomes an ionization source of the nighttime E region.

The excited hydrogen atoms emit photons mainly at two frequencies: Lyman α (121.6 nm) and Lyman β (102.6 nm). Both Lyman α and Lyman β are subject to small temporal variations due to magnetic activity and thermospheric temperatures. Owing to its relatively long wavelength Lyman α ionizes only NO molecules; the maximum absorption taking place where NO is abundant below 120 km. As a result, the ionization rates for Lyman α are very small in the upper E region. The maximum ionization by Lyman β is shown by *Ogawa and Tohmatsu* [1966] and *Strobel et al.* [1974] to occur in the altitude region between 90 to 110 km. Therefore, Lyman α and Lyman β are the main sources of nighttime ionization between 90 and 110 km. However, their contribution to the ionization above 120 km is negligible.

Ionization by helium radiation is mainly at two wavelengths: Helium I (58.4 nm) and Helium II (30.4 nm). Because of their relatively short wavelengths, they are easily absorbed by N_2, O_2 and O in the intermediate layer and, therefore, they are possible ionization sources in the altitude region between 120 and 200 km.

Below 110 km the UV radiation gives a satisfactory explanation of the electron-density profile. However, between the altitude of 120 and 200 km, the insufficient intensity and the poor correlation of UV radiation with magnetic activity cannot give a complete explanation of the electron density detected in that region. Therefore, other ionization sources must be sought.

2.2.2 *Transport and diffusion.* Diffusion of ambient electrons from the higher region (above 175 km) and the lower region (below 110 km) to the intermediate layer is prevented because of the two valleys at approximately 175 km and 110 km; the gradient of electron density in these valleys is zero. *Shen et al.* [1976] further concluded that vertical transport could supply no more than 10-20% of the required ionization in the nighttime E region. The diffusion and transport processes are not major factors in the equation of continuity [see *Voss and Smith*, 1977] but they may be important in establishing the shape of the electron-density profile in the altitude region 120 to 180 km.

The intermediate layer is caused by convergence of ionization due to the action of neutral winds forcing ionization across the earth's magnetic field. The explanation of the wind shear theory and the effect of transport and diffusion processes in the formation of the intermediate layer can be found in *Voss and Smith* [1977].

2.2.3 *Energetic particle precipitation.* Energetic particles originating in the sun interact with the magnetic field of the earth; some of them get trapped temporarily and form the radiation belts. These quasi-trapped particles constitute one possible source of ionization in the nighttime *E* region.

Protons from the ring current may constitute another source of ionization in the nighttime *E* region. Two mechanisms have been suggested which can bring the protons in the ring current to the lower atmosphere:

1. During a magnetic storm (i.e., when the Kp index is high) the compressed magnetic field of the earth forces the ring current to move inward. The gyrating protons in the ring current interact with the ambient electrons in the plasmasphere and become unstable. Some of the unstable protons are injected along the earth's magnetic field lines into the nighttime *E* region at midlatitudes and constitute an ionization source in that region of atmosphere [*Cornwall*, 1971].

2. Protons in the ring current are neutralized becoming high energy hydrogen atoms which can travel across the magnetic field lines into the atmosphere of the earth where they are re-ionized [*Moritz*, 1972]. However, this double-charge-exchange mechanism is important only in the vicinity of the equator and is probably not a significant process for the midlatitude experiment described in this report.

The altitude region in which the energetic particles are most effective in ionizing the neutral atmosphere is determined by their energy spectrum and their pitch-angle distribution. Furthermore, the particle energy spectrum varies with pitch angle and with altitude. Therefore, the information on the pitch-angle distribution of the energetic particles is very important in the experiment described in the subsequent chapters. The ionization rate in the nighttime *E* region due to energetic particles can be calculated from the particle flux, energy spectrum, pitch-angle distribution and the quantum efficiency of neutral constituent interactions. The calculation of the ionization rate is described in more detail in *Voss and Smith* [1974].

3. THE TIME-SHARING DATA-ACQUISITION SYSTEM

3.1 *General Description*

A data-acquisition system in general extracts information from the incoming signal which is supplied by the transducer and converts it to a form which can be processed by computers or microprocessors. In general the input of a data-acquisition system is an analog signal and the output is a digital code.

Usually the speed of the computer or microprocessor in processing the data is much faster than the speed that the individual channel can supply it. Therefore, in order to take advantage of the computational power of the micro-processor and the slow input data rate of the individual channels, several data channels are time-multiplexed to a single conversion channel and the result is a time-sharing data-acquisition system.

The general schematic of a four-channel data-acquisition system is shown in Figure 3.1. In this, continuous signals from transducers are sampled, multiplexed, digitized and encoded; the output signals are digital codes. Each code carries the information of an individual sample plus the address of the channel from which the sample was obtained. The codes are then processed through the interface circuit to the digital signal processor. The analog signal processor is usually a special function circuit such as logarithmic amplifier, square or sine function converter, which serves the purpose of dynamic range compression and signal-to-noise enhancement.

3.2 *Time-Sharing Multiplexing*

As shown in Figure 3.1, the sampling as well as the multiplexing are controlled by the timing programmer. Therefore by adjusting the timing pro-grammer, one can control the multiplexing so that the amount of data obtained from each channel can be regulated according to the data rate of the channels to the importance of one data channel compared with the others and to the regularity of the data in each channel. Multiplexing in any of the methods described above is called random-access multiplexing. On the other hand, if the multiplexer is controlled so that the channels are accessed sequentially, the result is a sequential multiplexing system. The sequential multiplexing system yields an output which consists of equal information obtained from each channel while a random-access multiplexing system gives one which consists of optimized information from the data channels.

One can also control the sampling signal to optimize the throughput of the system by multiplexing more channels to the main conversion channel.
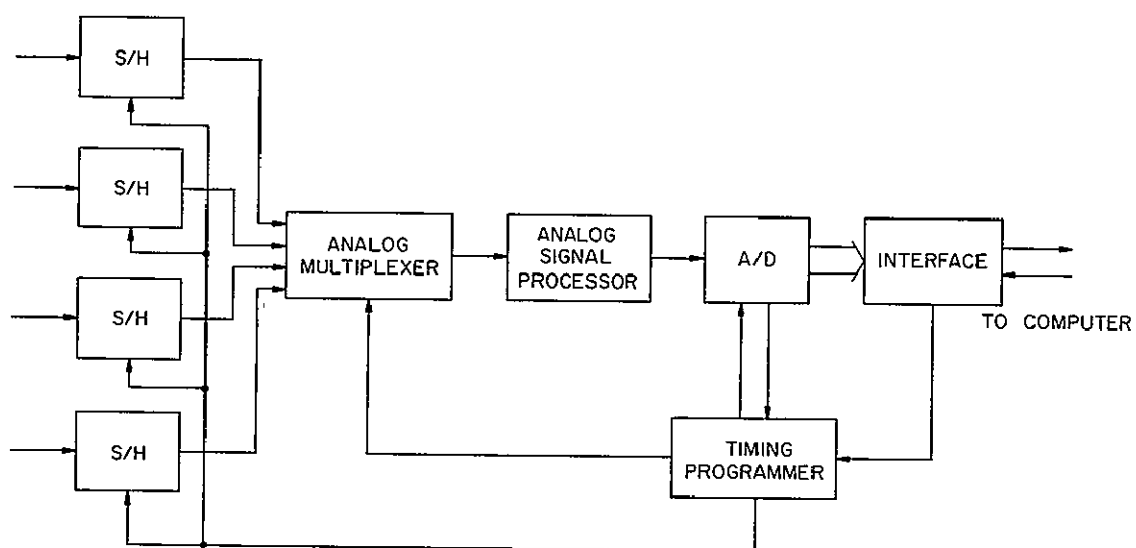
Figure 3.1   A general schematic of a four-channel time-sharing
             data-acquisition system.

3.3 *System Distribution between Analog and Digital Circuits*

As mentioned in Section 3.1, the input of the data-acquisition system is analog and the output is digital, therefore, the circuit of the system can be distributed between analog and digital. In order to show the flexibility of circuit distribution in a data-acquisition system, two extreme examples will be considered. In Figure 3.2 the input signal from the transducers are immediately digitized. As a result dynamic range compression and noise reduction are performed by a digital circuit. As shown in the figure, dynamic range compression is done by a digital function converter which usually is a read-only-memory serving as a look-up table. Digital filtering, not shown in the figure, is usually done by a software program inside the microprocessor. In Figure 3.3, on the other hand, range compression and signal conditioning are done by an analog circuit. As a result analog circuits dominate in this system.

The distribution of the circuit is determined not only by the basic constraints of circuit design, such as cost function, application environment and input-output factors, but also by the general characteristics of analog and digital circuits.

Digital and analog circuits are, generally, not replaceable by one anothe However, some specific data processing can be done by an analog circuit faster and cheaper than by a digital circuit. On the other hand, the information carried by the analog signals is more easily distorted by electrical noise than that carried by digital signals. Moreover, analog circuits usually have more stability problems than digital circuits. Therefore, in designing the circuit of a data-acquisition system, these characteristics of analog and digital circuits must be taken into account.

3.4 *Noise and Noise Immunity*

In this section the origin of noise in a data-acquisition system is investigated. The procedure used in the design of the system to improve the noise immunity of the system is then described.

In general, noise in a system falls into three categories:

1. Induced noise – undesired signal picked up from the environment and from the other data channels.

2. Inherent noise – noise generated by the circuit elements inside the system.

3. Transmitted noise – noise introduced by the transducer.
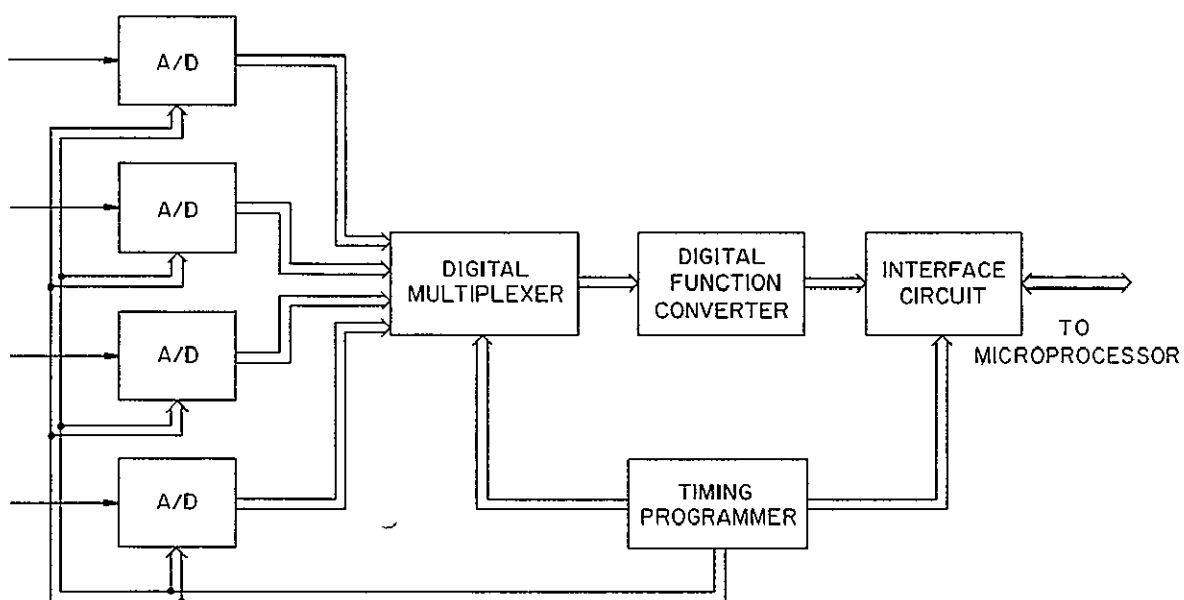
Figure 3.2 A data-acquisition system with predominantly digital
circuits. Double lines represent data buses.
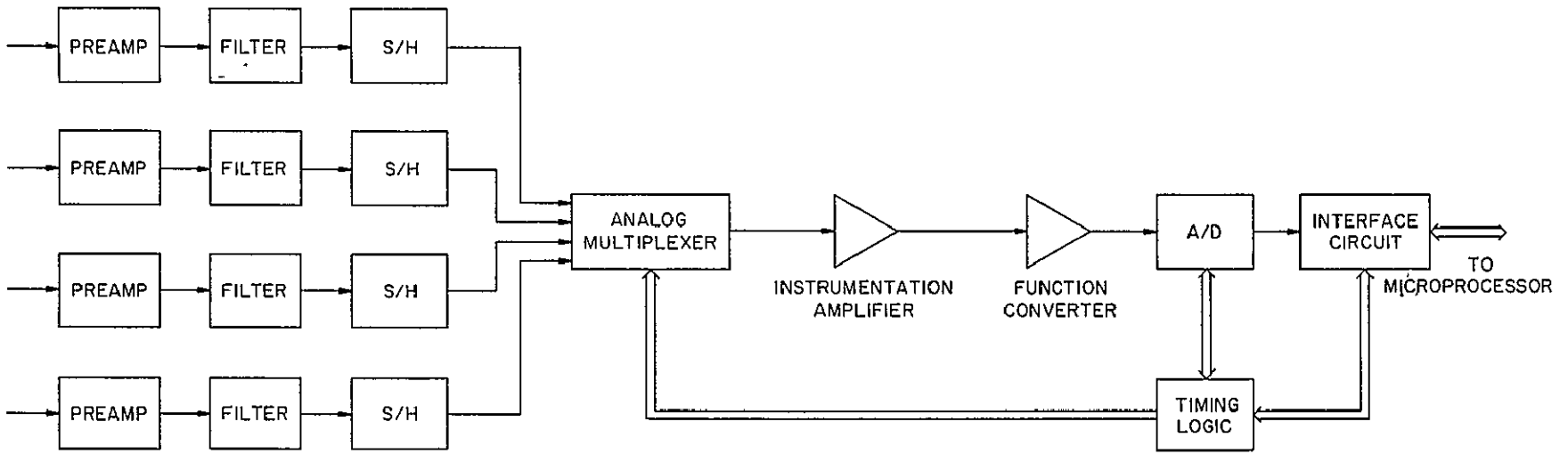
Figure 3.3 A data-acquisition system with predominantly analog circuits.

The noise immunity of a system refers to the level of noise under which a system can process its data properly with little loss of information. Knowing the origin of the noise, approaches can be taken through the design of the system to improve the noise immunity. By shielding the input transmission lines, using differential instead of single-ended input and by balancing the input impedance of the data channels, the noise immunity of the system against induced noise can be improved. By preamplification and filtering, the signal-to-noise ratio of the input can be improved and, therefore, the transmitted noise can be reduced. Finally by using low noise-level components and keeping the temperature of the system stable, the inherent noise can be minimized.

3.5 *Accuracy of the Output Data*

The accuracy of the data acquired depends mainly on the circuit processing it. In the following, several important circuit performance factors which have significant effect on the accuracy of the output data are briefly discussed:

1. The capability of the input stage to accurately acquire the information from the input signal. For example, consider the input stage of a data-acquisition system to be an operational amplifier which operates in the differential mode so as to sense the difference of the voltage between the two input terminals: in this case, the common mode rejection ratio and the offset voltage level of the op-amp are important to the accuracy of the data acquired.

2. The linearity of the analog circuit. If the analog data acquired are processed by some analog circuit, such as an instrumentation amplifier before they are converted into digital data, then the input-output linearity of the instrumentation amplifier is important to the accuracy of the output data. In the case of a logarithmic or a trigonometric function converter, the precision of conversion is important.

3. The performance of the analog multiplexer. Since an analog multiplexer consists of both analog and digital circuits, some interaction between the analog and digital circuit is unavoidable. This internal interaction together with external effects (such as channel-on and -off impedance, fluctuation of power supply voltage, input source impedance and stray capacitance) tend to introduce error in the multiplexed analog data. More details on the operation of analog multiplexers in data processing will be given in the next chapter.

4. Propagation delay of digital circuits. The main limitation on the switching speed of digital circuits is propagation delay. If the switching speed of the digital circuit in a data-acquisition system cannot keep up with the input data rate, information will be lost. Therefore, in designing the system, the switching speed of the digital circuit must be faster than the expected data rate.

5. Quantization error. Error is introduced when an analog signal is converted into digital data by an analog-to-digital converter; the error is called the quantization uncertainty. The amount of error is with $\pm\frac{1}{2}$ LSB (least significant bit value) of the A/D converter.

Therefore, a data-acquisition system processes data with a certain amount of error and minimizing it is the main concern in the design of the system.

4. THE PULSE-HEIGHT ANALYZER

4.1 *Introduction*

The pulse-height analyzer is basically a data-acquisition system. The input system and the general arrangement of the pulse-height analyzer are described in this chapter.

The two primary constraints in designing the system are circuit size and input factors. For the system considered here, space available in the payload is limited. As a result the size of the system is restricted to a 4" x 4" printed-circuit board in the payload of a Nike Apache rocket. The other constraint is imposed by the input transducers since they determine the signals which are the input to the system.

4.2 *The Input System*

The transducers in each of the rocket payloads consist of six solid-state detectors, an electrostatic analyzer and a magnetometer.

4.2.1 *The solid-state detectors.* The energetic particle spectrometers used in the two rocket payloads comprise a group of so-called surface-barrier solid-state detectors (Ortec Inc.). The two types of surface-barrier detectors used in this project are shown in Figure 4.1; one type uses gold on n-type silicon, the other uses aluminum on p-type silicon. The use of the two types simultaneously allows a determination of the type of energetic particle (i.e., electron or heavier).

Each surface-barrier detector has a 300 μm depletion depth and a sensitive area of 50 mm^2. When an energetic particle hits the sensitivity area, it propagates through the depletion region, losing its energy to the lattice electrons in the semiconductor and lifting them from the valence band into the conduction band. The resulting electron-hole pairs are then rapidly swept out by the high electric field which is created inside the depletion region by the external reverse-bias voltage. A pulse of current is produced; the total charge is proportional to the energy of the particle. Consequently, by calibrating the solid-state detectors properly [*Voss and Smith,* 1974], the energy spectrum of the energetic particle can be determined.

The energy lost by the particle in the metal surface layer does not contribute to the output current and the energy required for a particle to penetrate through the metal determines the threshold energy of the detector. Therefore, the threshold energy level of a detector is established by the thickness w and the nature (gold or aluminum) of the metal layer. Also the
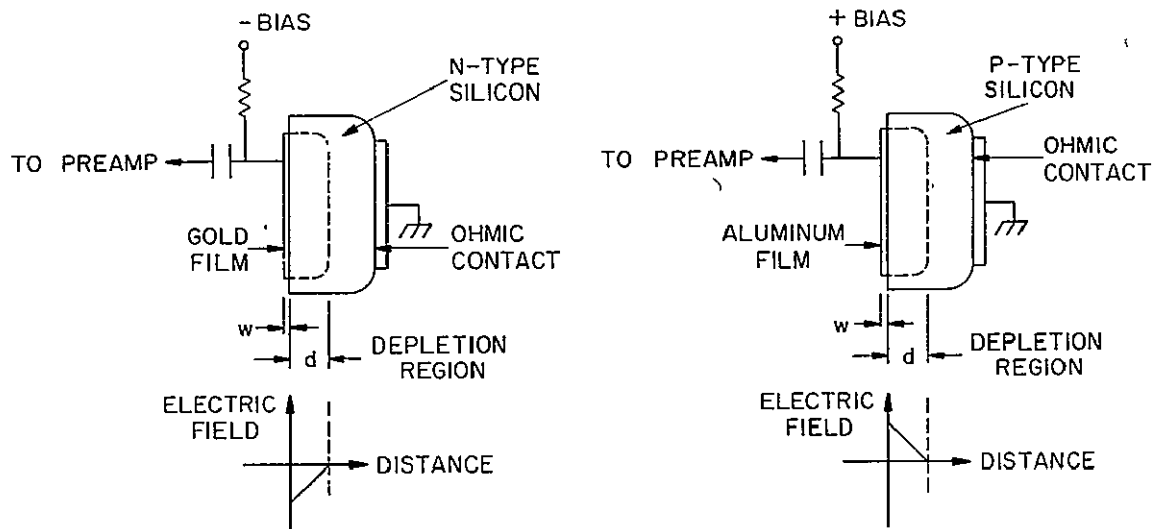
Figure 4.1   Two types of surface-barrier semiconductor detectors
and their bias circuits.

energy lost by a particle outside the depletion region does not significantly contribute to the output current. The energy required for a particle to penetrate through the depletion region determines the highest energy that can be detected.

The six solid-state detectors in Nike Apaches 14.542 and 14.543 have different threshold and maximum energy levels so that they can be used to analyze energetic particles over a wide energy spectrum. Also by mounting them at different angles in the rockets, some information on the pitch-angle distribution of the energetic particles can be obtained. The important characteristics of the detectors in the rockets are listed in Table 4.1. Note that the two payloads are not identical; this is because 14.542 is to be launched at dusk and 14.543 near midnight.

The equivalent circuit model of the solid-state detector is shown in Figure 4.2 [*Voss and Smith*, 1974]. In the diagram, $i_p(t)$ represents the current pulse introduced by an energetic particle; I_L is the leakage current of the detector which is also the reverse saturation current of the diode; C_p is the depletion layer capacitance; R_p is the equivalent resistance of the depletion region; C_s and R_s are the series capacitance and resistance of the semiconductor material, Z is the (ohmic) contact impedance and C_w is the capacitance of the connector.

4.2.2 *The electrostatic analyzer*. The electrostatic analyzer (ESA) is designed so that it can detect energetic particles in the low energy spectrum (0.9 to 14 keV). In this range the solid-state detectors cannot be used because of their high threshold energy levels.

The schematic of the ESA and its supporting electronics is shown in Figure 4.3. The voltage between the two cylindrical parallel plates is swept logarithmically from 200 to 3000 V in six steps, for each polarity alternately. Energetic particles coming in the collimator are either deflected into the multiplier or to the plates. The deflection depends on the energy and charge (positive or negative) of the particle as well as the polarity of the plate voltage. The particles deflected to the plates have no effect on the output data. The plate voltage sweep is controlled by the magnetometer signal such that the duration of one voltage step equals the period of the magnetometer signal which in turn indicates one revolution of the rocket.

The multiplier amplifies the charge of the particle and the preamplifier converts this charge into a current pulse. The amplitude of the pulse depends

Table 4.1   University of Illinois solid-state detector experiments.

Designation†	Geometrical Factor (cm² ster)	Front Surface Material (µg cm⁻²)	Look Angle from Spin Axis (deg**)	Energy Range (keV**)		Energy Channels (logarithmic)	Pitch Angle Sectors	Comments
				Electrons	Protons			
EPS 1 U	0 05	40-Au	90	>10	>15	12	15	High Resolution Detectors Energetic Particle Identification
EPS 1 D	0 05	40-Au	90	>150	>15	12	15	Electron Broom Magnet CWEF*
EPS 2 U	0 05	100-Al	90	>12	>55	11	15	For Energetic Particle Identification, CWEF
EPS 3 U	0 05	40-Al(Au)	45	>10	>25 (15)	12	15	Precipitated Flux
EPS 3 D	0.05	40-Al(Au)	135	>10	>25 (15)	12	15	Backscattered Flux
EPS 4 UD	0 05	40-Al	90	>10	>25	12	15	CWEF and Ion Mass Determination

* Comparison with earlier flights
** Parentheses for Nike Apache 14 543 only
† U indicates ascent and D indicates descent
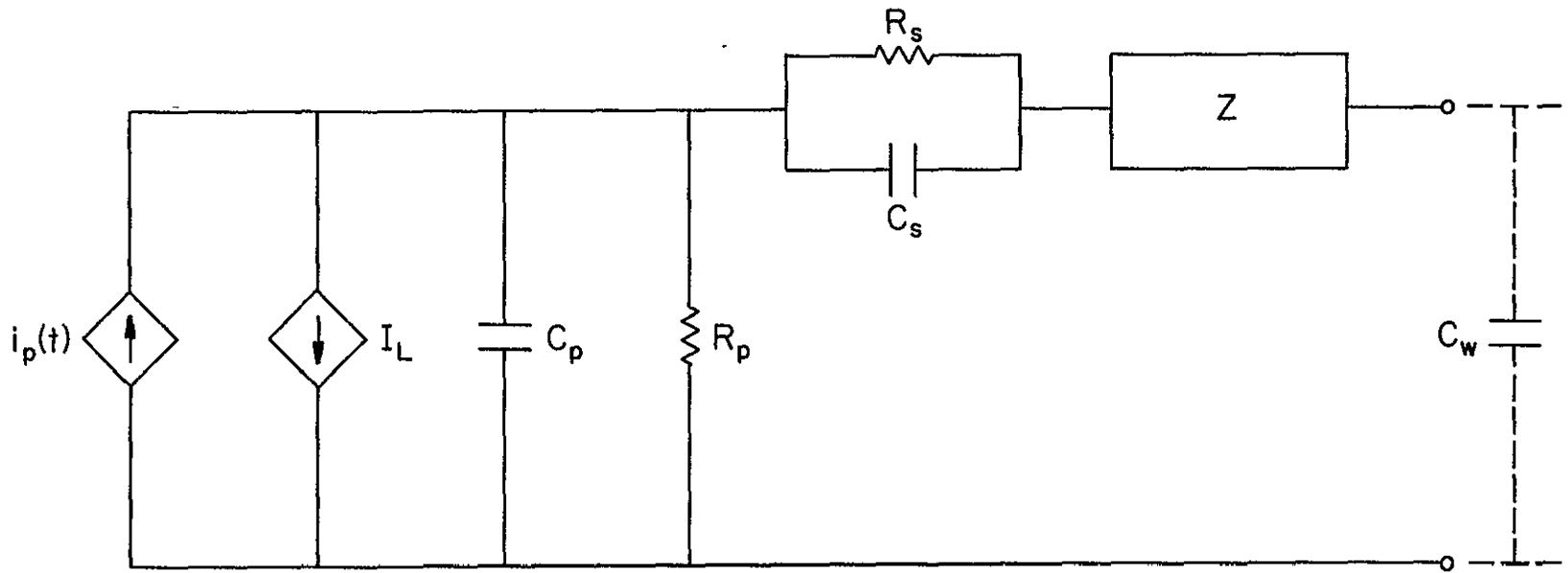
Figure 4.2   Equivalent circuit model of a solid-state detector.
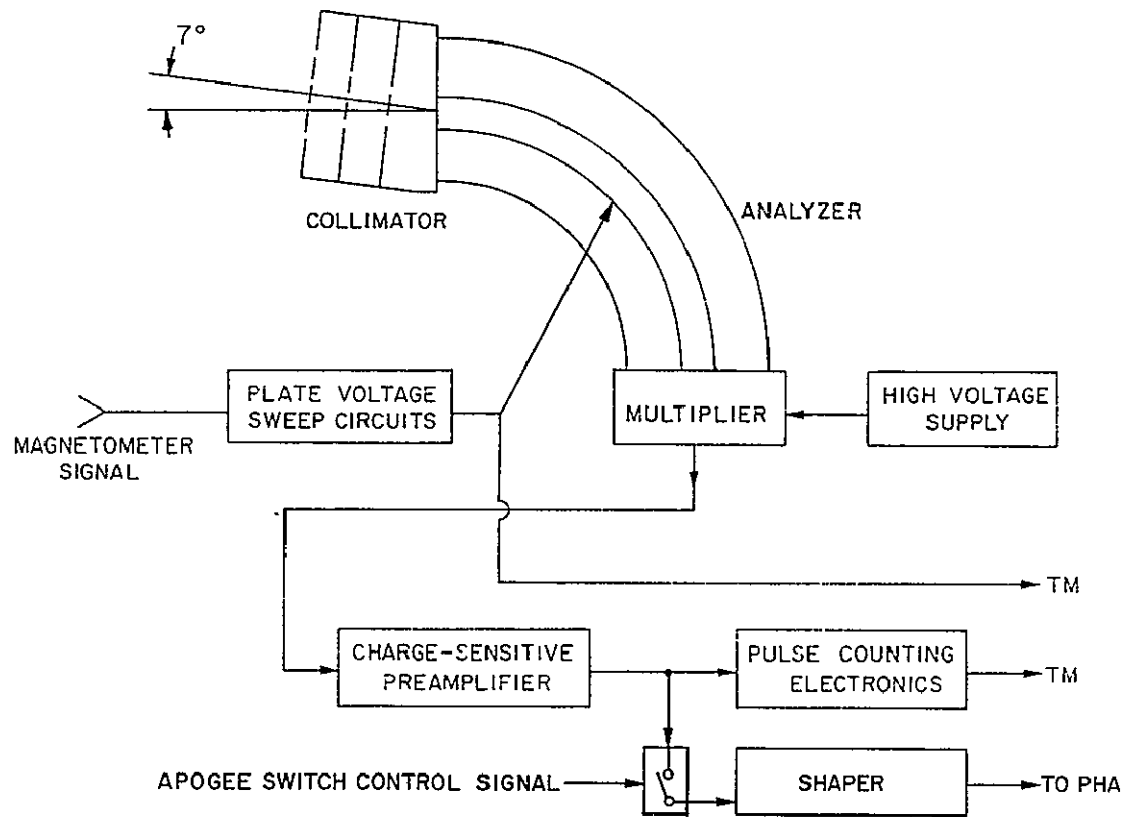
Figure 4.3 Electrostatic analyzer block diagram.

on the energy as well as the nature (protons, electrons or ions) of the particle. Therefore, different kinds of energetic particles yield different pulse-height distributions at the output of the multiplier. The information on the density, the energy spectrum and the nature of the energetic particles at certain altitudes can be obtained by analyzing the data from the ESA on the plate voltage, count rate and pulse-height distribution.

A detailed description of the electrostatic analyzer is contained in *Pozzi et al.* [1979].

4.2.3 *The preamplifiers and shapers.* The circuit of the preamplifier (Nucleometrics Inc.) and its equivalent model are shown in Figure 4.4. The main function of the preamplifier is to amplify the signal from the detectors (ESP and ESA) to a level suitable for data processing in the subsequent electronics. The preamplifier also minimizes the noise transmitted from the detectors and adjusts the time constant of the input pulse so that it matches the input conditions of the shaper. As shown in the equivalent circuit, R_2 and C_1 form the differentiator, C_2 forms the integrator and C_3 and R_c constitute a low-pass filter.

The equivalent circuit of a shaper is shown in Figure 4.5. The shaper consists of a differentiator, three integrators and a post-amplifier. The integrators are connected by high-pass RC filters. The time constants of the differentiator and integrators are chosen to be 1 µs which minimizes the transmitted noise. The output pulses of the shaper have amplitudes between 0 and 10 V. The output impedance is 100 kΩ. A typical output pulse of the shaper is shown in Figure 4.6. The typical output noise level with the solid-state detector is 100 mV rms. The output of the shaper is transmitted through a coaxial cable (60 cm long, 50 Ω characteristic impedance) to the input stage of the pulse-height analyzer.

The preamplifier and shaper are described in more detail in a report being prepared by K. L. Fries, H. D. Voss and L. G. Smith.

4.2.4 *The magnetometer.* The circuit diagram of the magnetometer (Schonstedt Instruments RAM-5C) is shown in Figure 4.7. Basically the instrument consists of an electronic unit and a field sensor. The sensor is made of a permalloy core with two sets of winding. When a magnetic field threads the permalloy core parallel with its long axis, a signal is induced. The induced signal has a frequency twice of that of the inducing field and has a dc offset of 2.4 V. The amplitude of the output signal is directly proportional to the
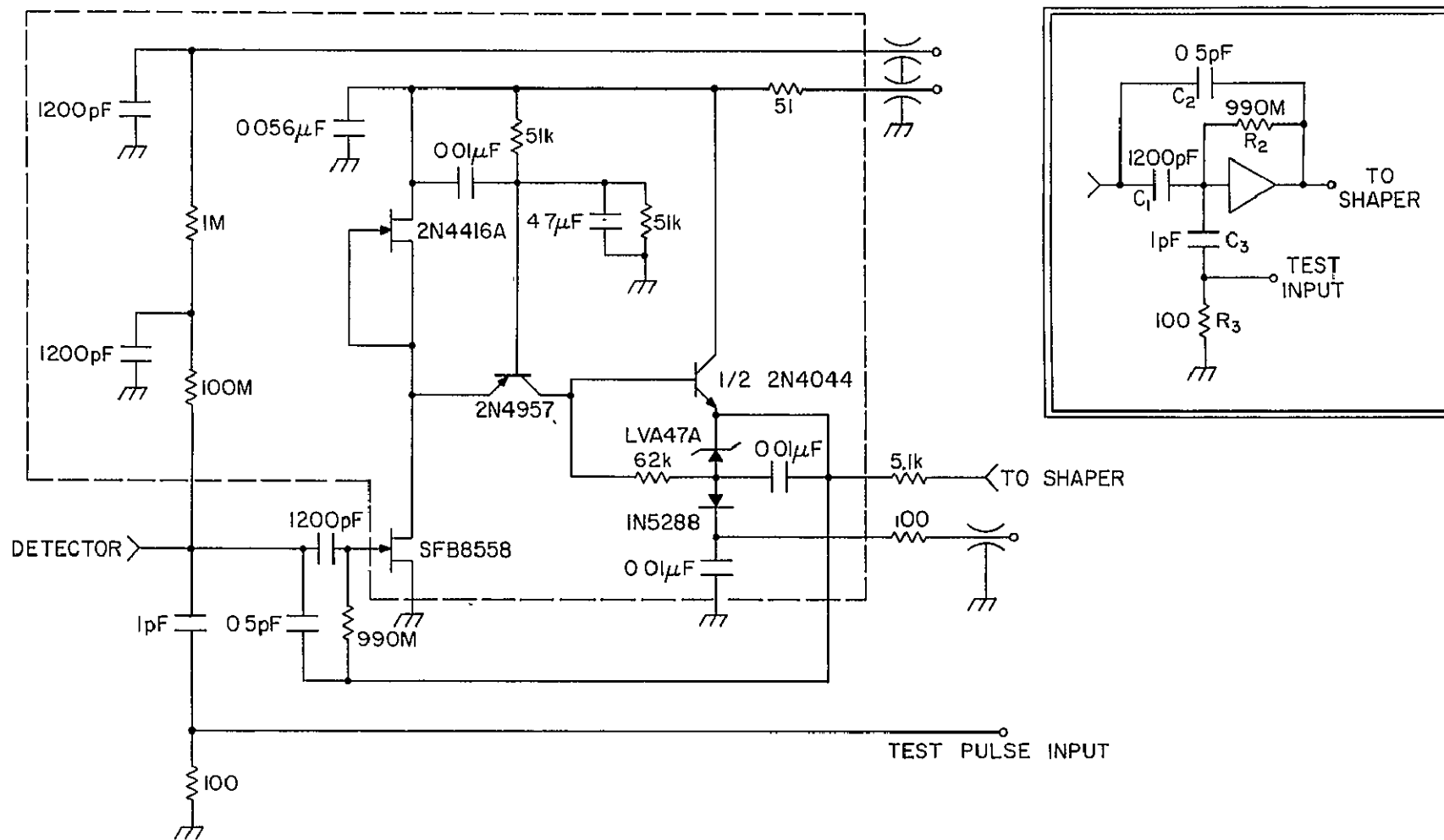
Figure 4.4 Preamplifier circuit diagram and its equivalent
          model. The circuit inside the dashed line is
          represented by the triangle in the equivalent
          circuit model.
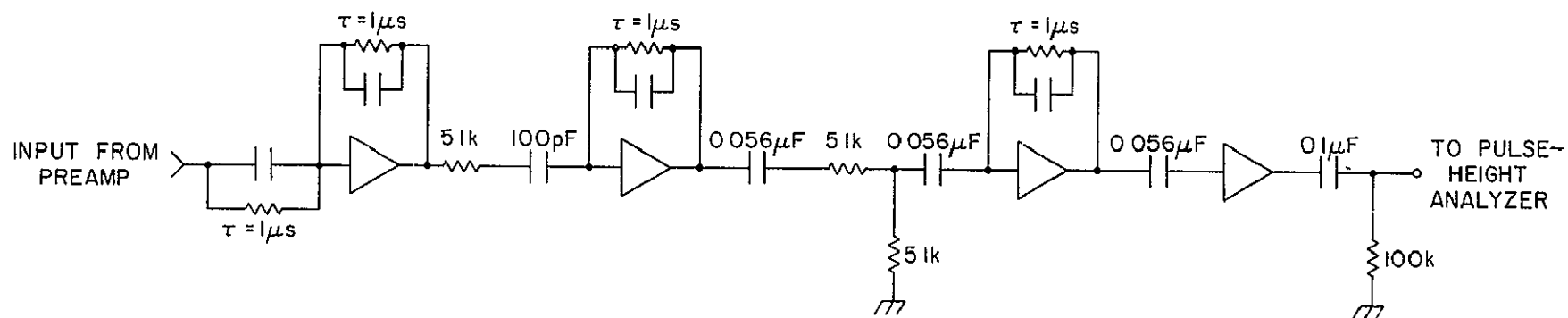
Figure 4.5 The equivalent circuit of the shaper.
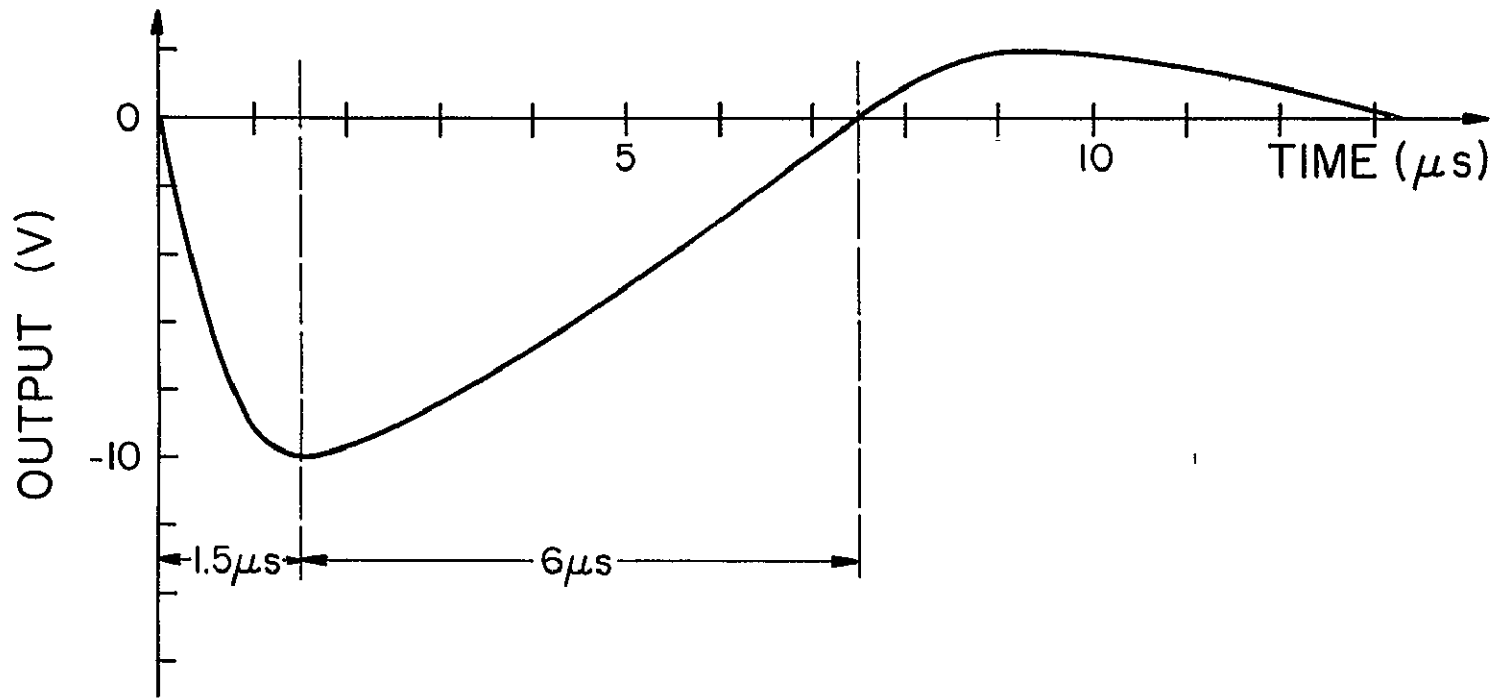
Figure 4.6 A typical output pulse of a shaper.

RAM-5C
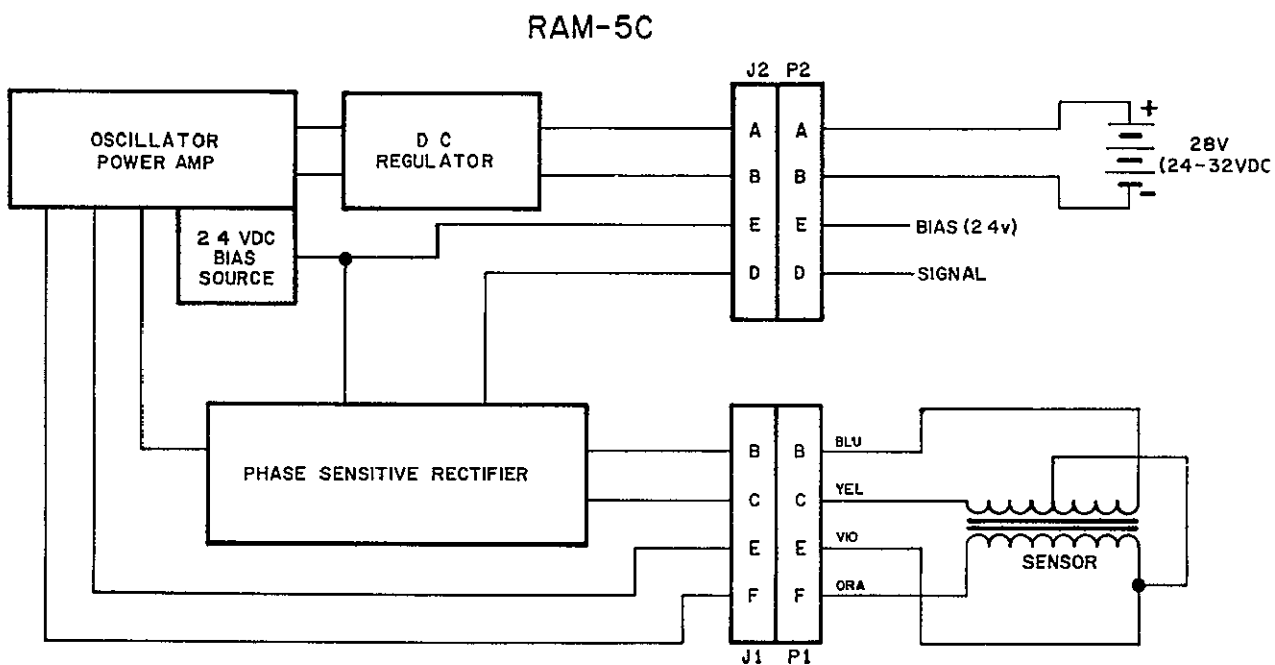
Figure 4.7 Circuit diagram of the magnetometer (Schonstedt Instrument Co.).

strength of the magnetic field.

In order to interpret the magnetometer signal properly, the spin and precession of the rocket during the flight and the magnetic field of the earth must be analyzed [see for example *Voss and Smith*, 1977]. We can deduce that if the precession of the rocket is small the magnetometer signal is a sine wave with small amplitude modulation; one period of the sine wave represents one spin of the rocket. Also, for the detectors oriented parallel to the magnetometer the pitch-angle distribution of the energetic particles can be obtained by appropriate use of the magnetometer signal.

4.3 *General Description of the Pulse-Height Analyzer*

The input system to the PHA is summarized in Figure 4.8. Four shapers are used. Three of these are switched, at rocket apogee, from one preamplifier to another.

Two gold film solid-state detectors connected by an apogee switch occupy data channel #1 of the PHA. An aluminum film detector for high energy particle and the electrostatic analyzer occupy data channel #2. Data channel #3 is occupied by two aluminum film solid-state detectors of lower threshold energy level. The last channel is occupied by another aluminum film solid-state detector. The input sinusoidal signal from the magnetometer goes through another part of the system: the magnetometer signal analyzer.

The main function of the PHA is to take the amplitude of each input pulse and convert it into digital code. The other function of the system is to provide digital information on the period of the sinusoidal wave from the magnetometer. The block diagram of the pulse-height analyzer is shown in Figure 4.9. A brief description of the system is given here, the circuits of the individual building blocks will be discussed in the next chapter.

The inputs from the shapers to the PHA are negative pulses. Each pulse-height detector latches on to the peak of a pulse. A capacitor inside the pulse-height detector stores the peak voltage until it is multiplexed to the isolation amplifier. The function of the isolation amplifier is to improve the accuracy of the data acquired, mainly by providing a high impedance load to the capacitor.

It was originally planned to include logarithmic compression of the pulse amplitude for more efficient use of the telemetry system. Since the signal from the isolation amplifier is negative, an inverter is needed before the signal can be processed by the logarithmic amplifier. The output of the

27
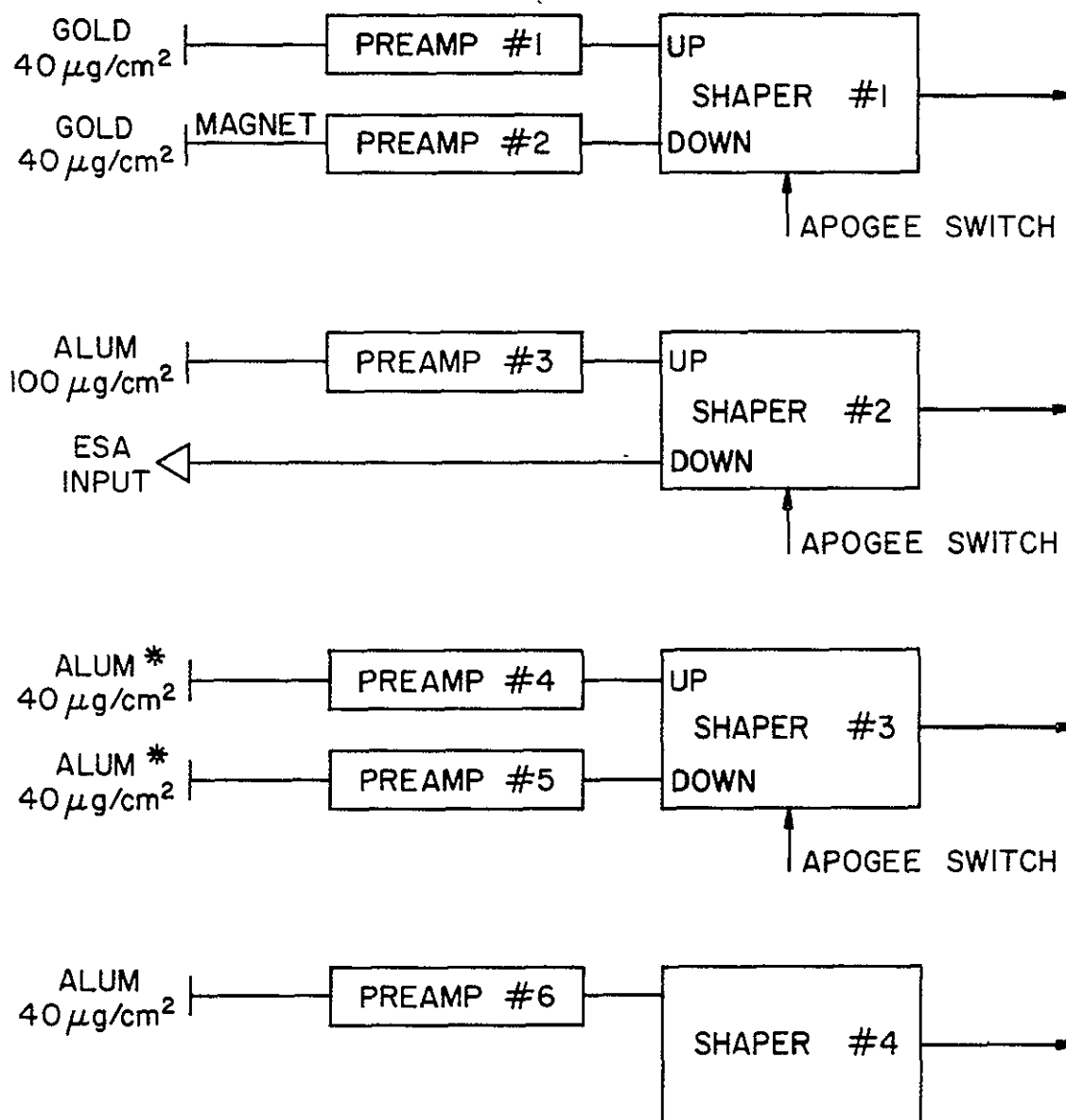
* IN 14 542   GOLD 40 μg/cm² IN 14 543

Figure 4.8   The input system of the PHA's in Nike Apache rockets
14.542 and 14.543.
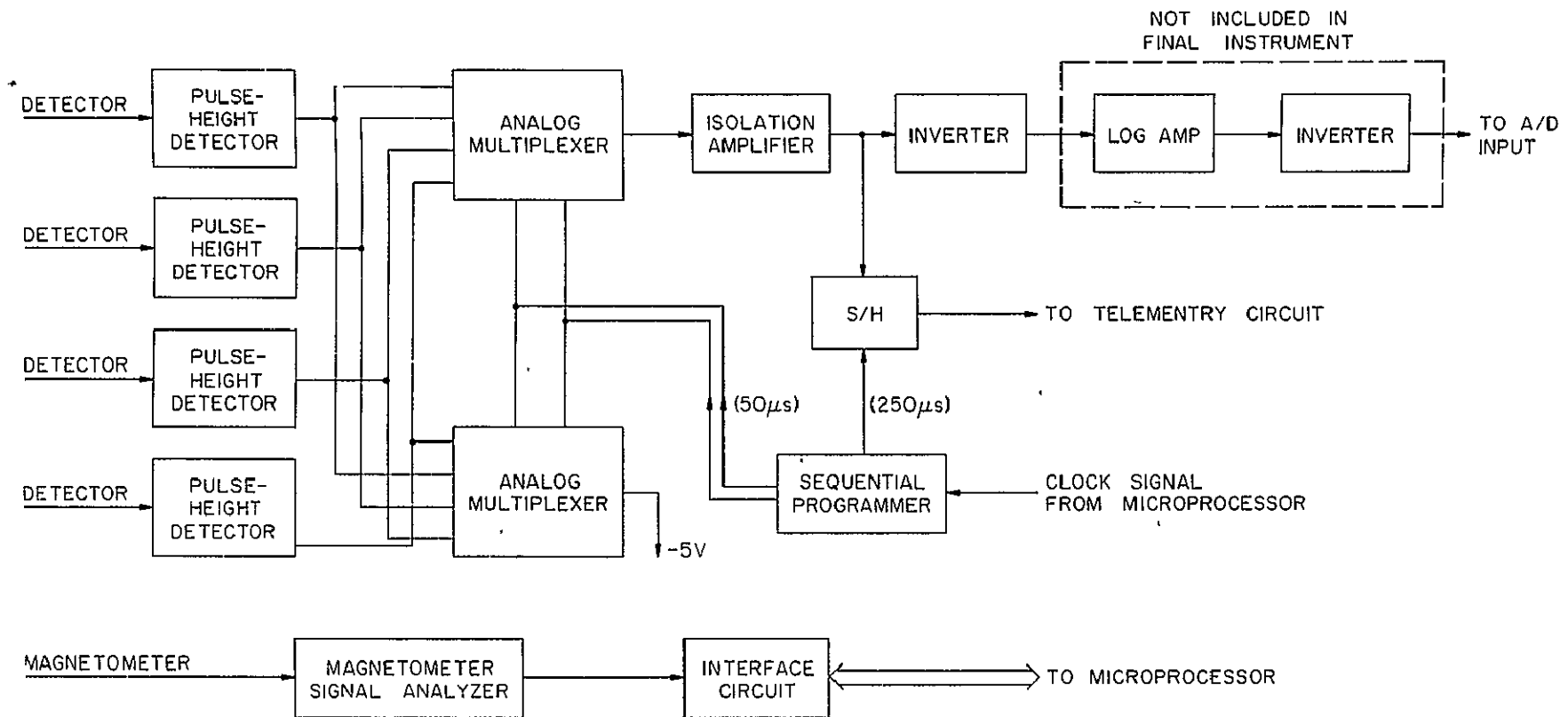
Figure 4.9 The block diagram of the pulse-height analyzer.

logarithmic amplifier is a negative voltage. The data from the log-amp are then converted back to a positive value by another inverter.

As will be discussed later, it proved impossible, in the time available, to develop a logarithmic amplifier of sufficient speed; the log-amp and the subsequent inverter were not included in the rocket payloads.

The positive analog data are then digitized by an A/D converter and the output digital data are interfaced to the Z-80 microprocessor experiment. The digital data obtained from the magnetometer signal analyzer are also interfaced to the microprocessor.

The magnetometer signal is a sinusoid with a frequency equal to the spin rate of the rocket. It is used in this experiment to identify the azimuth angle of the rocket. This allows the flux of the energetic particles to be examined as a function of pitch angle [see *Voss and Smith*, 1977].

The output of the magnetometer signal analyzer is a digital signal which represents the angular position of the rocket. Starting from a reference position the rotational position is divided into sectors on the basis of time increments of 10 ms, up to a maximum of 16 sectors. If the rotational period is smaller than 160 ms, the highest order sectors are empty or partially filled. For periods greater than 160 ms the lowest order sectors are re-entered. A detailed discussion is given in *Davis et al.* [1979].

The microprocessor analyzes the particle data and converts them back to analog data through a D/A converter. The analog data are then sent back to the ground station on channel 18 of the FM/FM telemetry system of the payload.

The sample-and-hold circuit in the pulse-height analyzer provides a backup to the microprocessor system. Even though channel H of the telemetry system is used, the data rate at the output of the multiplexer is too great to be transmitted directly. The sample-and-hold circuit is synchronized to the multiplexer so that every fifth pulse is read out. Since the multiplexer output consists of a sequence of four peak detectors, the output of the sample-and-hold preserves the sequence but at a data rate which is only 20% of that obtained from the microprocessor system.

The sequential programmer is the brain of the pulse-height analyzer. It controls the throughput rates of the system. It also provides correct timing for the proper functioning of individual building blocks in the system.

The input signal of the sequential programmer is a 2.5 MHz square wave generated by a crystal oscillator (clock). The clock also provides timing

for the microprocessor.

The output of the sequential programmer includes multiplexing control signals, an S/H control signal, a start-convert signal and a digital waveform for the microprocessor. The multiplexing signals determine the way that the input data channels are accessed. The S/H signal controls the sampling rate of the S/H. The start-convert signal provides correct timing to the A/D converter so that the analog signal is converted to digital at the right time.

5. THE ELECTRONIC CIRCUITS

5.1 *Introduction*

The amplitude (peak height) of the pulse from the transducers is measured in this data-acquisition system. The function of the PHA is to convert the amplitude of an input pulse into digital code.

The circuit of the main conversion channel is shown in Figure 5.1. It consists of peak detectors for four inputs, an analog multiplexer, an isolation amplifier, two inverters and a logarithmic amplifier. The design considerations of the circuit of the PHA are discussed in this chapter.

The output of the first stage of the PHA is to be a signal which represents the pulse amplitude. A peak detector turns out to be suitable for this purpose.

5.2 *The Peak Detector Circuit*

The general circuit of a peak detector with an isolation amplifier is shown in Figure 5.2. The input op-amp is a high slew-rate comparator. The diode blocks negative signals so that only positive voltages appear at the output. When the input voltage is higher than the output, the diode conducts and charges the capacitor until the voltage of the capacitor equals that of the input. If the input voltage is less than the output voltage, a negative voltage appears at the output of the comparator and the diode is turned off, leaving the output voltage unchanged. Therefore, the circuit is a positive peak detector. (A negative peak detector results if the polarity of the diode is reversed.) The second op-amp has high input impedance and low input bias current which isolates the capacitor from loading by the output. The other function of this op-amp is to increase the output current of the detector.

The peak detector of the PHA, shown in Figure 5.1, basically resembles the one in Figure 5.2. However, in Figure 5.1 the diode is missing (it will be seen later to be unnecessary) and the two operational amplifiers are separated by the analog multiplexer.

The LM239A quad comparator is chosen for the peak detector because of its small size and its use of a single power supply. The circuit of one of the four comparators is shown in Figure 5.3(a). By operating with one power supply, the comparator reacts only to one polarity of input voltage (i.e., the voltage between the positive and negative input terminals). For the other polarity of input voltage, the input transistors are cut off. Therefore,
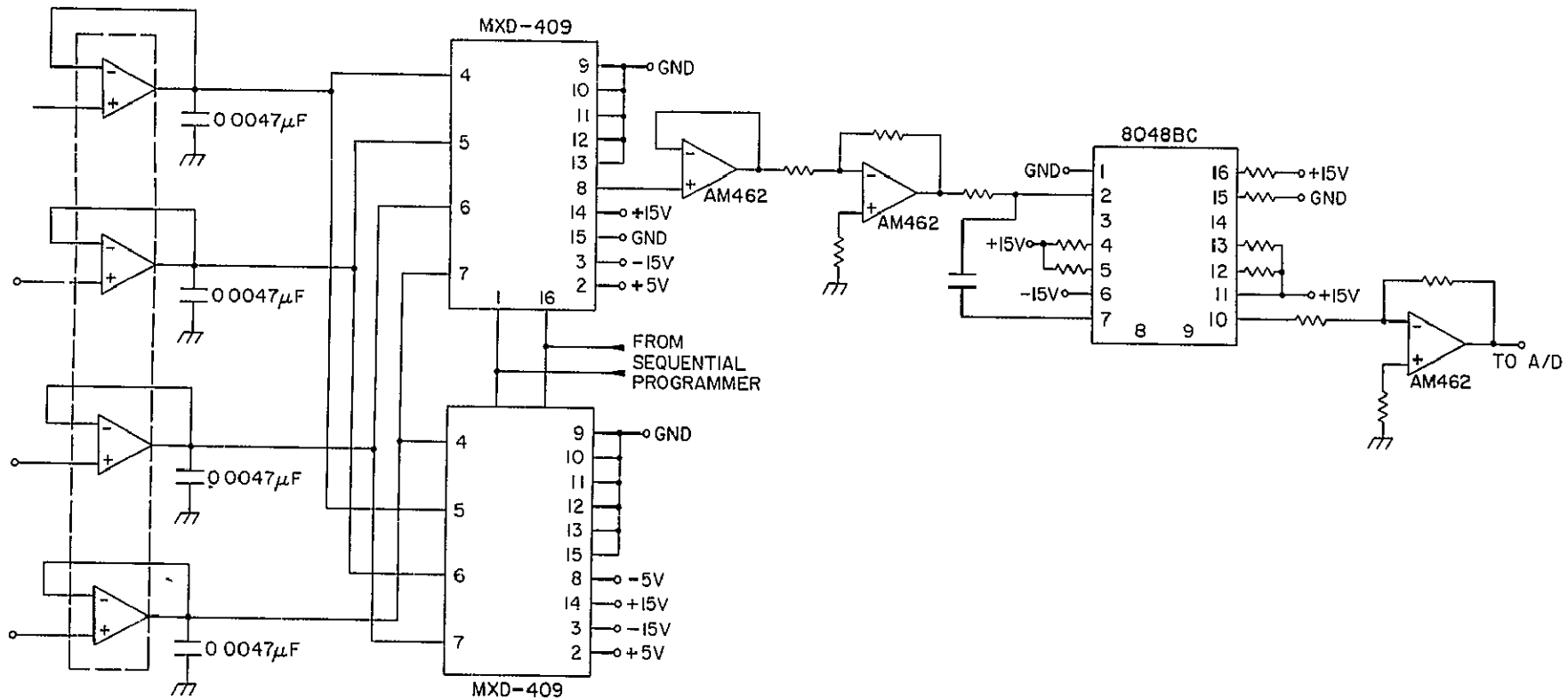
Figure 5.1 The main conversion channel.
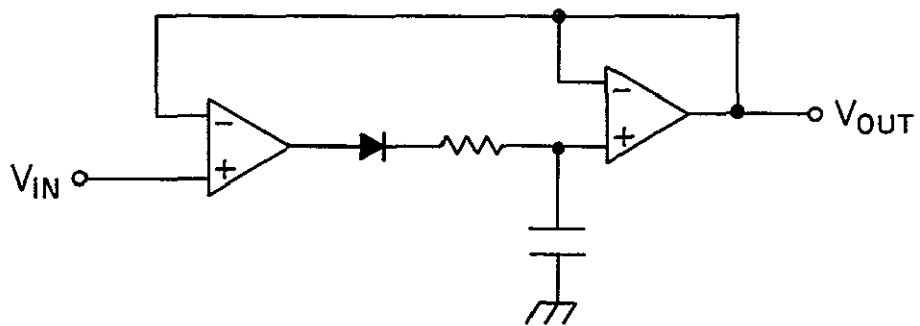
Figure 5.2 A positive peak detector including an isolation amplifier.

(a)

(b)

(c)

Figure 5.3 One of the four identical circuits of the LM239A quad
comparator is shown in (a). Circuit (b) shows ¼LM239A
used as a positive peak detector with Miller effect
compensation capacitor C_1. Circuit (c), also a positive
peak detector, uses a negative feedback capacitor C_2.

when operated with a positive power supply, the comparator has a non-zero output only when the voltage at the positive terminal is higher than the voltage at the negative terminal. As a result when this comparator is used in the peak detector, the diode of Figure 5.2 is not required. The maximum ratings and electrical characteristics of LM239A are listed in Table 5.1.

The shaper can output either negative or positive pulses, therefore, either a negative or a positive peak detector can be used. The positive peak detector was first chosen because an inverter can be eliminated in the main channel of the PHA (see Figure 5.1). However, as will now be explained, this turned out to be a poor choice; the final version uses a negative peak detector.

A positive peak detector using a $\frac{1}{4}$LM239A is shown in Figure 5.3(b). In the circuit, R_1 is the passive pull-up resistor. The npn 2N2222 transistor is added to increase the current gain of the comparator so that C_2 can be charged effectively. The voltage across the capacitor is reset by a second analog multiplexer. The reset time is 50 μs and the reset frequency is 5 kHz. However, because of the junction capacitance of the transistor and the capacitive load, C_2, additional phase shift is introduced to the feedback system. As a result, the system oscillates at low input frequencies (below 200 Hz). C_1 is, therefore, used as a phase-lag-compensation capacitor to stabilize the system. Alternatively, system stabilization can be achieved by increasing the value of C_2. However, C_1 is more effective than C_2 since C_1 uses the Miller effect of the transistor.

The crucial defect of the circuit is that, because of the compensation capacitor, the slew rate of the system is decreased dramatically. Consequently, input pulses of rise time less than 5 μs and of amplitude greater than 4 V cannot be peak-detected accurately. Different-methods of feedback compensation have been tried; the one that gives the best result is shown in Figure 5.3(c). In the circuit, the resistor R_3 is introduced to isolate the load capacitor C_3; C_2 provides negative feedback. Because of the isolation and the feedback capacitor, the Miller effect capacitance is reduced by 90% and the circuit is able to detect pulses of rise time greater than 3 μs and of amplitude.less than 7 V. However, the system is required to peak-detect pulses of 1.5 μs rise time and of 10 V amplitude. As a result, the positive peak detector was abandoned and a negative peak detector used.

Table 5.1 Absolute maximum ratings and electrical characteristics of LM239A (National Data Book)

Absolute Maximum Ratings

Supply Voltage, V^+	36 V_{DC} to ±18 V_{DC}
Differential Input Voltage	36 V_{DC}
Input Voltage	-0.3 V_{DC} to +36 V_{DC}
Power Dissipation (Note 1)	
Molded DIP (LM339AN)	570 mW
Cavity DIP (LM139AD, LM239AD & LM339AD)	900 mW
Flat Pack (LM139AF)	800 mW
Output Short-Circuit to GND (Note 2	Continuous
Operating Temperature Range	
LM339A	0°C to +70°C
LM239A	-25°C to +85°C
LM139A	-55°C to +125°C
Storage Temperature Range	-65°C to +150°C
Lead Temperature (Soldering, 10 s)	300°C

Electrical Characteristics

(V^+ = 15 V_{DC} and T_A = 25°C unless otherwise noted)

Parameter	Conditions	LM139A min	LM139A typ	LM139A max	LM239A, LM339A min	LM239A, LM339A typ	LM239A, LM339A max	Units
Input offset voltage	At output switch point, $V_0 \cong 1.4\ V_{DC}$, $V_{REF} = +1.4\ V_{DC}$ and $R_s = 0\Omega$		1	2		1	2	mV_{DC}
Input bias current (Note 3)	$I_{IN(+)}$ or $I_{IN(-)}$ with output in linear range		25	100		25	250	nA_{DC}
Input offset current	$I_{IN(+)} -I_{IN(-)}$		3	25		5	50	nA_{DC}
Input common-mode voltage range (Note 4)				V^+-1.5			V^+-1.5	V_{DC}
Supply current	$R_L = \infty$ on all comparators		8	2		.8	2	mA_{DC}
Voltage gain	R_L = 15 kΩ		200			200		V/mV
Response time (Note 5)	V_{RL} = 5.0 V_{DC} and R_L = 5.1 kΩ		1.3			1.3		μs
Output sink current	$V_{IN(-)} = +1\ V_{DC}$, $V_{IN(+)} = 0$ and $V_0 \leq +1\ 5\ V_{DC}$	6	16		6	16		mA_{DC}
Saturation voltage	$V_{IN(-)} = +1\ V_{DC}$, $V_{IN(+)} = 0$ and $I_{SINK} = 3\ mA$		200	400		200	400	mV_{DC}
Output leakage current	$V_{IN(+)} = +1\ V_{DC}$, $V_{IN(+)} = 0$ and $V_{OUT} = 5\ V_{DC}$		0.1			.1		nA_{DC}

Note 1: For operating at high temperatures, the LM339A must be derated based on a +125°C maximum junction temperature and a thermal resistance of 175°C/W which applies for the device soldered in a printed circuit board, operating in a still air ambient. The LM239A and LM139A must be derated based on a +150°C maximum junction temperature The low bias dissipation and the ON-OFF characteristic of the outputs keeps the chip dissipation very small (Pd $\leq$ 100 mW), provided the output transistors are allowed to saturate.

Note 2   Short circuits from the output to V^+ can cause excessive heating and eventual destruction   The maximum output current is approximately 20 mA independent of the magnitude of V^+

Note 3. The direction of the input current is out of the IC due to the PNP input stage This current is essentially constant, independent of the state of the output so no loading change exists on the reference or input lines.

Note 4· The input common-mode voltage or either input signal voltage should not be allowed to go negative by more than 0.3 V. The upper end of the common-mode voltage range is V^+ -15 V, but either or both inputs can go to +30 V_{DC} without damage

Note 5   The response time specified is for a 100 mV input step with 5 mV overdrive. For larger overdrive signals 300 ns can be obtained, see typical performance characteristics section.

The negative peak detector shown in Figure 5.1 consists of a ¼LM239A and a capacitor. The isolation of the output capacitor is provided by the analog multiplexer when the data channel is off and by the isolation amplifier when the channel is on. The isolation will be discussed in more detail in the next two sections. The chosen value of the capacitor is 0.0047 µF. How this capacitor affects the performance of the detector will be discussed later in this section. The detector is able to peak-detect accurately input pulses of 1.5 µs at frequencies below 1 MHz and of amplitude between -1 and -7.5 V.

One feature of the detector is that it has an offset voltage of -1 V. As shown in Figure 5.3(a) the output transistor of the comparator has an open collector. With a negative voltage supply and the transistor Q_7 cut off, the output stage of the comparator is as shown in Figure 5.4. The output transistor is working in its active region instead of being cut off as it would be when working with a positive supply. Consequently, an offset of -1 V appears at the output. This offset voltage cannot be eliminated by connecting an external bias voltage to the input terminals (as is usually done on op-amps with two power supplies) because of the single supply. Any input pulse of amplitude less than -1 V can hardly be identified from noise; therefore, the -1 V offset is tolerable in the system.

As mentioned above, the value of the output capacitor of the peak detector affects both the detection speed and the accuracy of the output data. The bigger the capacitor, the longer it will take to charge and, hence, the slower will be the detection speed. If the rise time of an input pulse is faster than the detection speed, the output of the detector will not give the correct information on the pulse height. Also, the bigger the capacitor, the larger is the decay constant. Since the function of the capacitor is to hold the peak voltage of the input pulse until this information is multiplexed to the next stage, this voltage is subject to change due to the decay constant of the capacitor. Therefore, the bigger the capacitor, the more accurate will be the output data. The 0.0047 µF capacitor gives the detector adequate detection speed while maximizing the decay constant.

5.3 *The Multiplexing and Resetting Circuit*

The MXD-409 analog multiplexer is chosen for the time-division multiplexing because of its small size (16-pin DIP) and its short settling time (less than 2 µs). The resetting of the four output capacitors of the peak
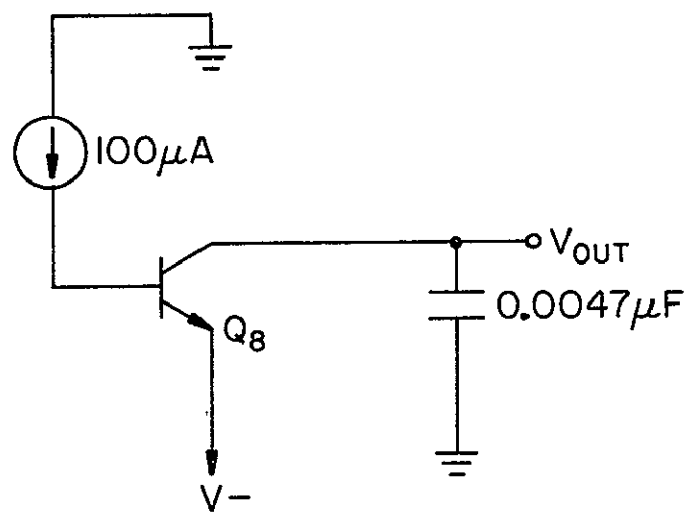
Figure 5.4 The output stage of the LM239 with a negative
power supply and with the input stage cut-off.

detectors is done by another MXD-409. The on-channel impedance (2 kΩ) together with the input capacitor gives a reset time constant of 9.4 μs. By connecting the output terminal of the resetting multiplexer to the -5 V supply instead of ground, the resetting time is shortened by at least a factor of 3. The multiplexers are controlled by the sequential programmer so that the channels are accessed sequentially. The access time and reset time is 50 μs for each channel. Each channel is reset immediately after it is accessed; the break-before-make feature of the multiplexers make this kind of resetting possible. The characteristics of MXD-409 are listed in Table 5.2.

As mentioned in the previous section, the multiplexers provide channel-off isolation to the output capacitors of the peak detectors. With 30 pA channel-off input leakage and very high (essentially infinite) channel-off input impedance, the multiplexers provide good input isolation.

In the rest of this section, major sources of error in the multiplexed data, such as input-output leakages and crosstalk, are analyzed.

Not only does leakage affect the voltage stored in the output capacitor of the peak detector, it also introduces error into the multiplexed output signal. Three kinds of leakage are of major concern: channel-off input leakage, channel-off output leakage and channel-on leakage. These are introduced by the CMOS transmission gates inside the multiplexer. They are the result of the reverse saturation current of the protecting diode, and the drain-to-source, gate-to-drain, gate-to-source, substrate-to-drain and substrate-to-source leakage of individual MOS elements constituting the transmission gate. The channel-off input leakage is the major source of input error. The other two leakages, on the other hand, cause errors mainly on the output. These will now be discussed in detail.

The circuit indicating the leakage currents is shown in Figure 5.5 where the substrate leakage is neglected. Assuming that channel #1 is on and the other channels are off, the error voltage can be calculated as follows:

$$Ve(\text{CH1}) = \frac{(R_{on1} + R_{s1} + 1\text{k})R_{in}}{R_{on1} + R_{s1} + R_{in} + 1\text{k}} \{2I_{gs(on)} + 3[2I_{gs(off)}I_{ds(off)}]\}$$

$$(5.1)$$

R_{on1} represents the channel-on impedance. R_{s1} is the source impedance. R_{in} represents the equivalent input impedance of the following stage. The subscripts (on) and (off) indicate channel-on and channel-off, respectively.

Table 5.2 Electrical characteristics of MXD-409*
(Datel Systems, Inc.)

Analog Inputs

Number of channels	4
Type	Differential
Input voltage range	±15 V
Input overvoltage, max.	±│Vs +20 V│
Channel ON resistance	1.5 K
Channel ON resistance, max., 0 to 70°C	2.0 K
Channel OFF input leakage	30 pA
Channel OFF output leakage	1.0 nA .
Channel ON leakage	100 pA
Channel OFF input capacitance	5 pF
Channel OFF output capacitance	12 pF

Digital Inputs

Logic "0" threshold, max.	+0.8 V
Logic "1" threshold, min. (TTL)	+4.0 V
Logic "1" threshold, min. (CMOS)	----
Input current, max., high or low	5 µA
Channel address coding	2 bits
Channel inhibit, all channels OFF	Logic "0"

Performance

Transfer error, max.	.01%
Crosstalk, 10 kHz	-86 dB
Common mode rejection -	120 dB
Settling time, 20 V step to 0.1%	2 µs
Settling time, 20 V step to .01%	5 µs
Turn ON time	500 ns
Turn OFF time	300 ns
Break-before-make delay	80 ns
Inhibit/enable delay	300 ns

Power Requirement

Rated power supply voltage	±15 VDC
Power supply voltage range	±5 to ±20 V
Quiescent current, max.	+5, -2 mA
Power consumption, 10 kHz sampling	7.5 mW

Physical-Environmental

Operating temperature range	0 to 70°C
Storage temperature range	-65 to +150°C
Package	16 pin DIP
Package dissipation, max.	725 mW

*Specifications -- Typical at 25°C, +15 V supplies,
R source < 1 K, unless otherwise noted.
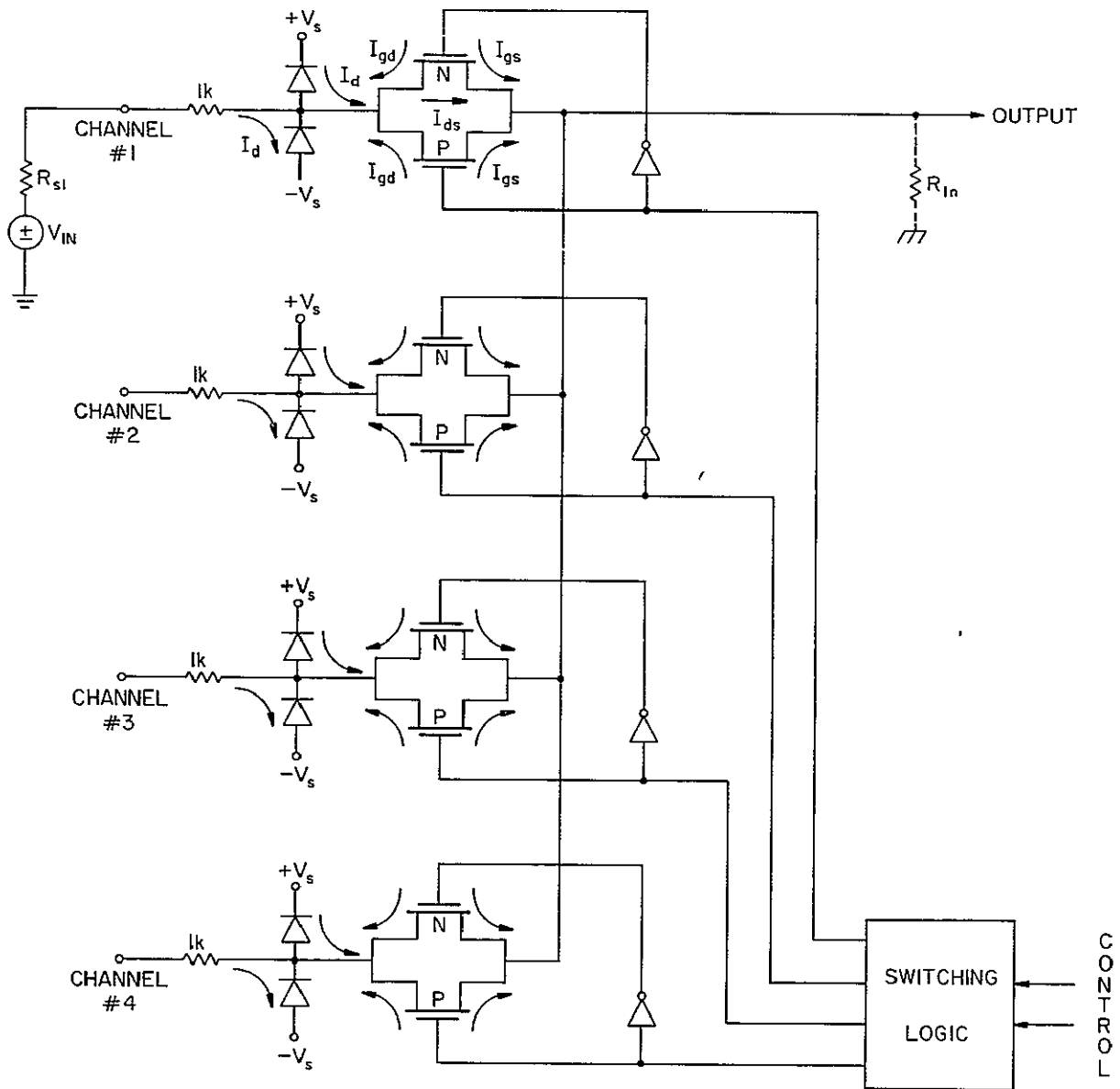
Figure 5.5   Leakage currents in the MXD-409.

In this expression the gate-to-drain leakages are neglected and the leakage currents of the protecting diodes are assumed to cancel with each other. If we put the channel-off output leakage (I_{on}) equal to $2I_{gs(on)}$, equation (5.1) can be simplified to

$$Ve(\text{CH1}) = \frac{(R_{on1} + R_{s1} + \text{1k})R_{in}}{R_{on1} + R_{s1} + R_{in} + \text{1k}} (I_{on} + 3I_{off})$$ (5.2)

With $R_{in} \gg R_{on1} + \text{1k} + R_{s1}$

$$Ve(\text{CH1}) \simeq (R_{on1} + R_{s1} + \text{1k})(I_{on} + 3I_{off})$$

Using values from Table 5.3

$$Ve(\text{CH1}) \simeq [100 \times 10^{-12} + 3 \times 1 \times 10^{-9}][2 \times 10^3 + 0 \cdot 1 \times 10^3 + 10^3] = 9 \cdot 61 \times 10^{-6}$$

(5.3)

where the output resistance of the peak detector, R_s, is assumed to be 100 Ω. From equation (5.3), we see that the error on the data induced by the leakage currents is negligible.

Another source of error in analog multiplexing is crosstalk. However, as shown in Table 5.2, this source of error is negligible inside the multiplexers. Crosstalk external to the multiplexers is minimized by shielding the inputs of the detectors and by good printed-circuit-board layout.

5.4 *The Isolation Amplifier and the Inverters*

The AM462-2 op-amp is chosen for the isolation amplifier and the two negative inverters in the main conversion channel. This op-amp is small (an 8-pin metal can); moreover, it has a very high input impedance (300 MΩ), wide bandwidth (1 MHz at unity gain) and high slew rate (35 V/μs). With these characteristics, the op-amp is especially suitable for the data-acquisition system. The electrical characteristics of the op-amp is listed in Table 5.3.

As mentioned in the last two sections, the channel-on isolation of the peak detector output capacitors is provided by the isolation amplifier. With an input bias current of 5 nA and input impedance of 300 MΩ, good isolation is obtained. Also, the transfer accuracy of the multiplexer depends on both the output impedance of the comparator and the input impedance of the isolation amplifier. The circuit used to determine the accuracy of the data transfer is shown in Figure 5.6: V_D is the data voltage, R_o is the output

Table 5.3 Specifications of AM462 (Datel Systems, Inc.)

Typical @25°C
V_S = ±15 VDC
R_L = 2 kΩ unless otherwise noted

Differential
Bipolar input
150 K DC Gain
100 MHz f_t

Input Characteristics

Differential Voltage	±12 V max
Common Mode Voltage Operating Range	±11 V min
Common Mode Rejection Ratio (V_{CM} = ±5 VDC)	100 db typ 74 db min
Input Impedance (Differential)	300 MΩ typ 40 MΩ min
Voltage Offset Initial (without external trim Adjustable to zero with trim)	3 mV typ @25°C 5 mV max @25°C 7 mV max 0 to 75°C
Voltage Offset vs Temp	15 μV/°C, 0 to 75°C
Zero Adjust (optional)	100 kΩ trimpot
Bias Current $= \left\|\frac{1^+ + 1^-}{2}\right\|$	5 nA typ @25°C 25 nA max @25°C 40 nA max 0 to 75°C
Offset Current $= \|1^+ - 1^-\|$	5 nA typ @25°C 25 nA max @25°C 40 nA max 0 to 75°C
Equivalent Input Noise (10 Hz to 10 kHz, zero source impedance)	2 μV ram

Output Characteristics

Voltage (Full Temperature Range)	±10 V min
Current, Continuous (V_{OUT} = ±10 V)	±10 mA min
Current, Peak	Short circuit protected (output to common) current limited

Gain and Frequency Response

Open loop gain, DC V_{OUT} = ±10 V	150 K V/V typ 80 K V/V min
Full Power Bandwidth	600 kHz typ 320 kHz min
Slew Rate (V_{OUT} = ±10 V step transition, C_L = 50 pF)	35 V/μs typ 20 V/μs min
Unity Gain, small signal	100 MHz (closed loop gain = 100, C_L = 50 pF)
Stability	Ext comp required at closed loop gain < 5
Settling time to within 0 1% (V_{OUT} = ±10 V step, C_L = 50 pF, A_v = +3)	

Power Supply

Operating Voltage	
Max Voltage Difference between V_S^+ and V_S^- terminals	45 V max
Absolute Max Internal Power Dissipation	
Quiescent Current	3 mA typ 4 mA max

Temperature Range

Operating, rated specs	
Storage	
Package	AM-462-1 TO-116 AM-462-2 TO-99
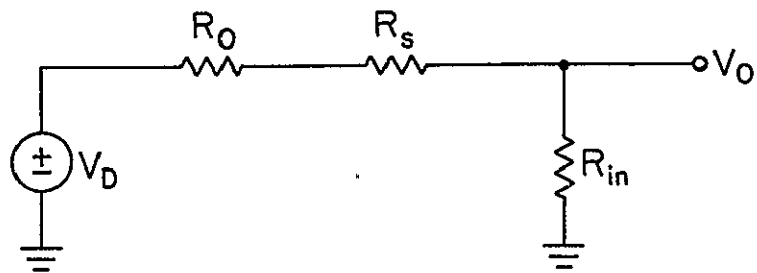
Figure 5.6 Circuit used to calculate the data-
transfer error.

resistance of the comparator (typical value 100 Ω); R_s is the channel-on resistance of the multiplexer (maximum value 2 kΩ); R_{in} is the input impedance of the op-amp (typical value 300 MΩ); and V_o is the voltage of the data transferred. V_o can be calculated from the following equation

$$V_o = \left[\frac{R_{in}}{R_o + R_s + R_{in}} \right] V_D$$

If $R_{in} \gg R_o + R_s$, i.e., $R_{in} \gg 2.1$ kΩ, then $V_o \approx V_D$ and we have a close-to-perfect transfer. Therefore, the bigger the input impedance of the op-amp, the better will be the accuracy of the data transferred. With R_{in} equal to 300 MΩ, the error introduced during the data transfer is negligible.

Three AM462's are used in the system. The one used for isolation has the configuration of a voltage follower; the other two are negative inverters with gain of 1 and 5, respectively. With 1 MHz bandwidth and 35 V/μs slew rate, stabilization of the op-amp with a feedback loop is easily obtained without significantly reducing the speed of the op-amp. A 100 pF compensation capacitor is used and the corresponding frequency response graph is shown in Figure 5.7.

5.5 The Logarithmic Amplifier

The 8048 logarithmic amplifier is chosen for dynamic range compression. By using dynamic range compression, output resolution of the A/D converter can be improved by trading off linear scale output for non-linearity. Moreover, the pulse-height distribution of different kinds of energetic particles are nearly logarithmic. Therefore, by using a log-amp, the output will become nearly linear.

The basic circuit of 8048 is shown in Figure 5.8. Q_1 and Q_2 are matched transistors, therefore, the output voltage of the log-amp does not depend on the reverse saturation currents. A_1 and A_2 are high gain op-amps. The expression for the output voltage in terms of the input current (I_{in}) and circuit parameters is given by equation (5.4)

$$V_{out} = \left[\frac{R_1 + R_2}{R_2} \right] \frac{kT}{q} \ln \left[\frac{I_{C1}}{I_{C2}} \right] = -2.303 \frac{kT}{q} \left[\frac{R_1 + R_2}{R_2} \right] \log_{10} \left[\frac{I_{in}}{I_{REF}} \right]$$

$$(5.4)$$

where k is Boltzmann's constant (1.38×10^{-23} J K^{-1}), T is the absolute temperature, and q is the electron charge (1.6×10^{-19} C). The thermistor, R_1,

Figure 5.7   Frequency responses of AM462 with
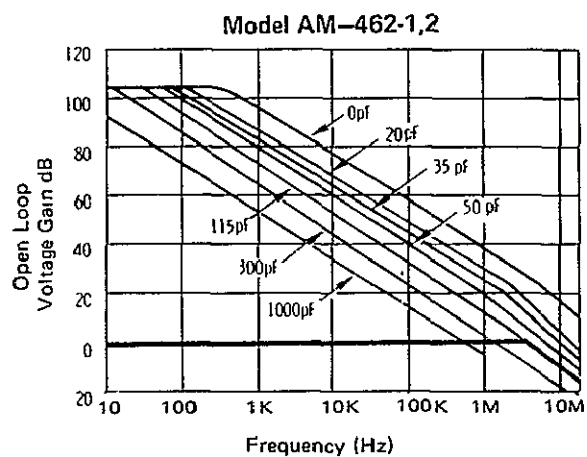different compensation capacitors.
The unity-gain (voltage follower)
response is indicated by the thick
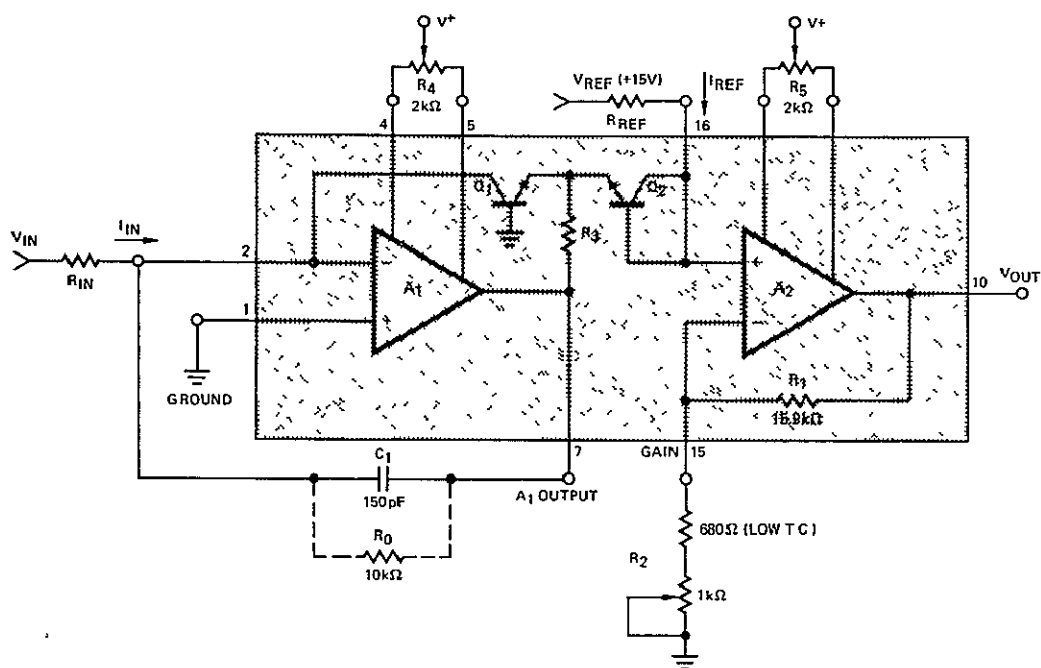line (Datel Systems, Inc.).

Figure 5.8   The 8048 offset and scale factor adjustments (from
            Intersil Semiconductor Products Catalog).

compensates the output voltage against changes due to temperature.

The log-amp was first designed to have an output scale of 10 V/decade for an input range of 1 to 10 V. However, in order to decrease the settling time, the scale was changed to 2 V/decade. The adjustment of the log-amp for these input and output requirements is shown in Figure 5.8. Basically, three kinds of adjustments are required: the offset adjustment, the zero (or origin) adjustment and the scale-factor adjustment.

The offset adjustment of A_1 is done by first connecting a resistor, R_o, across the input and output of A_1 and then adjusting R_4 while leaving the input open. The adjustment is made until the output voltage of A_1 is zero. R_o is removed after the adjustment.

The zero adjustment is controlled by R_{REF}, R_{in} and R_5. The input and output ranges require the output be set to zero for 1 V at the input. The adjustment is made as follows. First I_{in} and I_{REF} are set equal to 1 mA by putting R_{in} and R_{REF} equal to 1 kΩ and 15 kΩ, respectively; R_5 is then adjusted until V_{out} equals zero.

The output range adjustment is made by setting the input voltage equal to 10 V and then adjusting R_2 until V_{out} equals 2 V.

After these adjustments, the trimpots R_2, R_4 and R_5 are replaced by fixed resistors with corresponding values.

The stability of the log-amp is controlled by the compensation capacitor, C_1. However, C_1 also increases the settling time of the log-amp. The output waveform of the main conversion channel is shown in Figure 5.9. The output pulses, due to the settling time of the log-amp, have long rise and fall times. The log-amp was eventually abandoned because the settling time was somewhat longer than the access time (50 μs) of each channel. The output waveform of the main conversion channel without the log-amp and the output inverter is shown in Figure 5.10. Also shown in these figures are the corresponding output waveforms of the sample-and-hold circuit which will be discussed in the next section.

5.6 *The Sample-and-Hold Circuit*

The sample-and-hold (S/H) in the data-acquisition system is used as a backup to the microprocessor system. The sampling rate is adjusted to 1/5 of the multiplexing rate, so that 20% of the data can still be sent back in case of failure of the microprocessor. The sampling rate corresponds to the maximum data rate that the telemetry circuit can send.

Figure 5.9   Output waveforms of the sample and hold (upper trace)
and the main conversion channel (lower trace) resulting
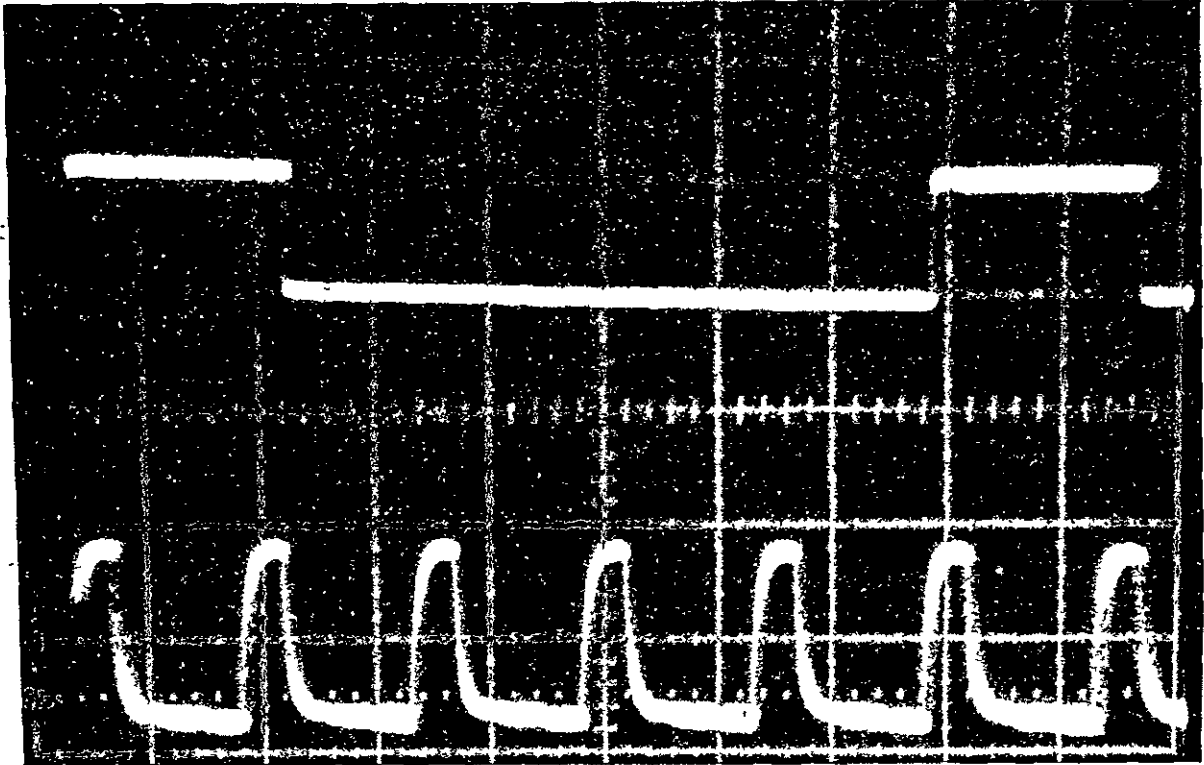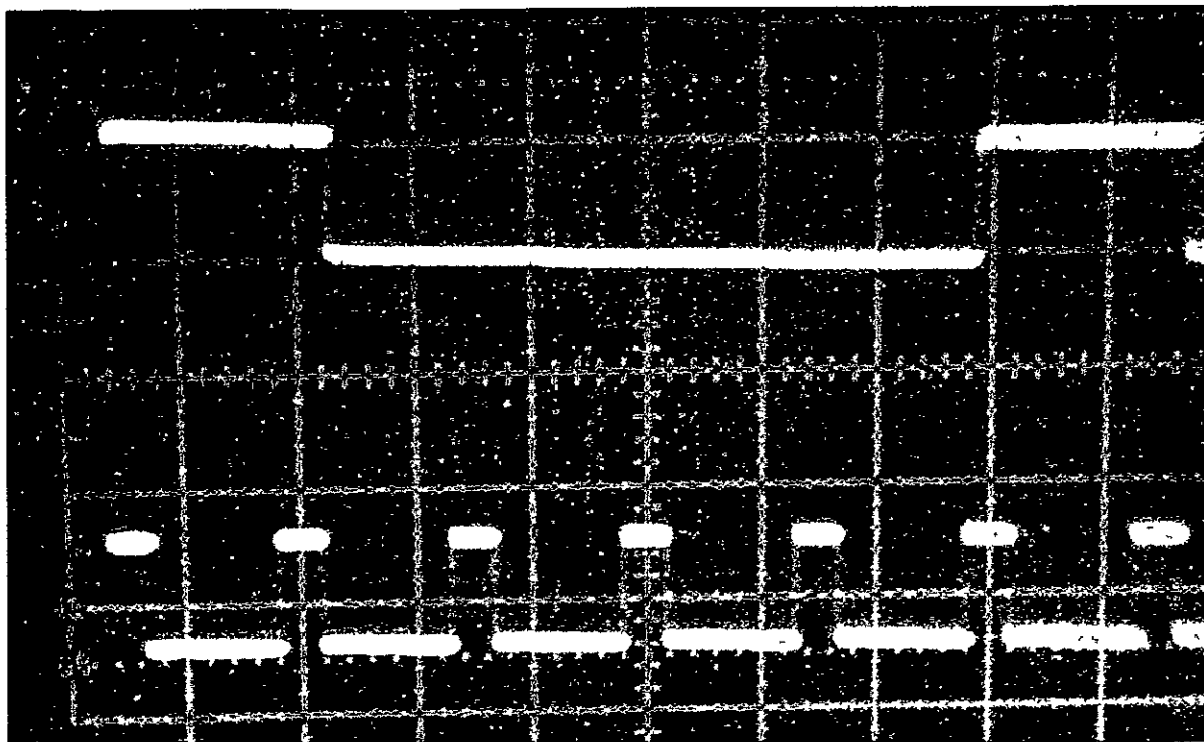from a 10 V input signal at channel #1 and 0 V at the
other three channels.

Figure 5.10   Output waveforms of the sample and hold (upper trace) and the main conversion channel (lower trace) without the log-amp and the output inverter. The outputs result from a 10 V signal applied at channel #1 and 0 V at the other three channels.

LH0053C is chosen for the S/H because of its small size (12-pin metal can) and its fast acquisition time (5 μs for 20 V). The maximum ratings and electrical characteristics are listed in Table 5.4. The circuit of the S/H using LH0053C is shown in Figure 5.11. In the diagram, op-amp A_1 is connected as a voltage follower. It provides high input impedance to the S/H so as to minimize the transfer error (see Section 5.3). It also provides current gain to the input signal so that the storage capacitor, C_2, can be charged more rapidly. Q_1 is a p-channel JFET; it is the switch controlling the sample-and-hold phase of the circuit. Op-amp A_2 is an inverter; it also provides isolation to the storage capacitor and small output impedance to minimize transfer error.

The selection of the storage capacitor affects the drift error on the output data. A high quality capacitor has less leakage current and, therefore, minimizes the drift error. Also, a larger value capacitor gives a larger output decay constant and hence introduces less drift error. However, the larger value capacitor also increases the acquisition time of the S/H. The storage capacitor in the circuit is chosen to be made of mylar and has a value 0.01 μF. With this capacitor, the acquisition time of the S/H is 1 μs.

5.7 *The Sequential Programmer*

The circuit of the sequential programmer, as shown in Figure 5.12, is composed of two SN74L393's and two SN74LS123's. Each SN74LS393 contains two binary counters and each SN74LS123 contains two monostable multivibrators (one-shots). One of the counters in SN74LS393(#2) is not used; one of the one-shots in SN74LS123(#1) is used in the magnetometer-signal analyzer which is described in the next section. Block schematics of the two chips are shown in Figures 5.13 and 5.14.

The access time of each input data channel is designed to be 50 μs and the channels are accessed sequentially. Therefore, the multiplexing signals are fixed to be 5 and 10 kHz. With the input clock signal of 2.5 MHz, frequency dividers of 256 and 512 are required. The two dividers are formed by three binary counters inside the two SN74LS393's; the outputs at pin 8 of chip #1 and pin 3 of chip #2 are square waves with frequencies of 9.8 kHz and 4.9 kHz, respectively. The waveforms combine to yield a switching time of 50 μs.

In order to minimize output error, the A/D converter is designed to convert signals at the middle of the access time of each channel. Also, the

Table 5.4 Maximum ratings and electrical characteristics of LH0053C (National Data Book)

Absolute Maximum Ratings

Supply Voltage (V^+ and V^-)	±18 V
Gate Input Voltage (V_6 and V_7)	±20 V
Analog Input Voltage (V_4)	±15 V
Input Current (I_8 and I_5)	±10 mA
Power Dissipation	1.5 W
Output Short Circuit Duration	Continuous
Operating Temperature Range	
LH0053	-55°C to +125°C
LH0053C	-25°C to +85°C
Storage Temperature Range	-65°C to +150°C
Lead Temperature (Soldering, 10 seconds)	300°C

Electrical Characteristics (Note 1)

Parameter	Conditions	Limits LH0053C min	typ	max	Units
Sample (Gate "0") Input Voltage				0.5	V
Sample (Gate "0) Input Current	$V_6 = 0.5$ V, $T_A = 25°C$ $V_6 = 0.5$			-5 0 -100	µA µA
Hold (Gate "1") Input Voltage		4.5			V
Hold (Gate "1") Input Current	$V_6 = 4.5$ V, $T_A = 25°C$ $V_6 = 4\ 5$ V			1 0 1 0	nA µA
Analog Input Voltage Range		±10	±11		V
Supply Current	$V_4 = 0$ V $V_6 = 0.5$ V		13	18	mA
Input Bias Current (I_4)	$V_4 = 0$ V, $T_A = 25°C$		150	500	nA
Input Resistance		9.0	10	11	kΩ
Analog Output Voltage Range	$R_L = 2\ 0$ k	±10	±12		V
Output Offset Voltage	$V_4 = 0$ V, $V_6 = 0\ 5$ V, $T_A = 25°C$ $V_4 = 0$ V, $V_6 = 0\ 5$ V		5 0	10 15	mV mV
Sample Accuracy (Note 2)	$V_4 = ±10$ V, $V_6 = 0\ 5$ V, $T_A = 25°C$		0.1	0.3	%
Aperture Time	$\Delta V_6 = 4.5$ V, $T_A = 25°C$		10	25	ns
Sample Acquisition Time	$V_4 = ±10$ V, $T_A = 25°C$, $C_F = 1000$ pF		8.0	15	µs
Sample Acquisition Time	$V_4 = ±10$ V, $T_A = 25°C$, $C_F = 100$ pF		4 0		µs
Output Slew Rate	$\Delta V_{IN} = ±10$ V, $T_A = 25°C$, $C_F = 1000$ pF		20		V/µs
Large Signal Bandwidth	$V_4 = ±10$ V, $T_A = 25°C$, $C_F = 1000$ pF			200	kHz
Leakage Current (Pin 5)	$V_4 = ±10$ V, $T_A = 25°C$ $V_4 = ±10$ V		10	50 3 0	pA nA
Drift Rate	$V_4 = ±10$ V, $T_A = 25°C$ $C_F = 1000$ pF		10	50	mV/s
Drift Rate	$V_4 = ±10$ V, $C_F = 1000$ pF			3 0	V/s
02 Switch ON Resistance	$V_7 = 0\ 5$ V, $I_8 = 1.0$ mA, $T_A = 25°C$		100	300	Ω

Note 1 Unless otherwise noted, these specifications apply for $V_S = ±15$ V, pin 9 grounded, a 1000 pF capacitor between pin 5 and pin 11, pin 3 shorted to pin 11, over the temperature range -55°C to +125°C for the LH0053 and -25°C to +85°C for the LH0053C All typical values are for $T_A = 25°C$

Note 2 Sample accuracy may be nulled by inserting a potentiometer in the feedback loop This compensates for source impedance and feedback resistor tolerances

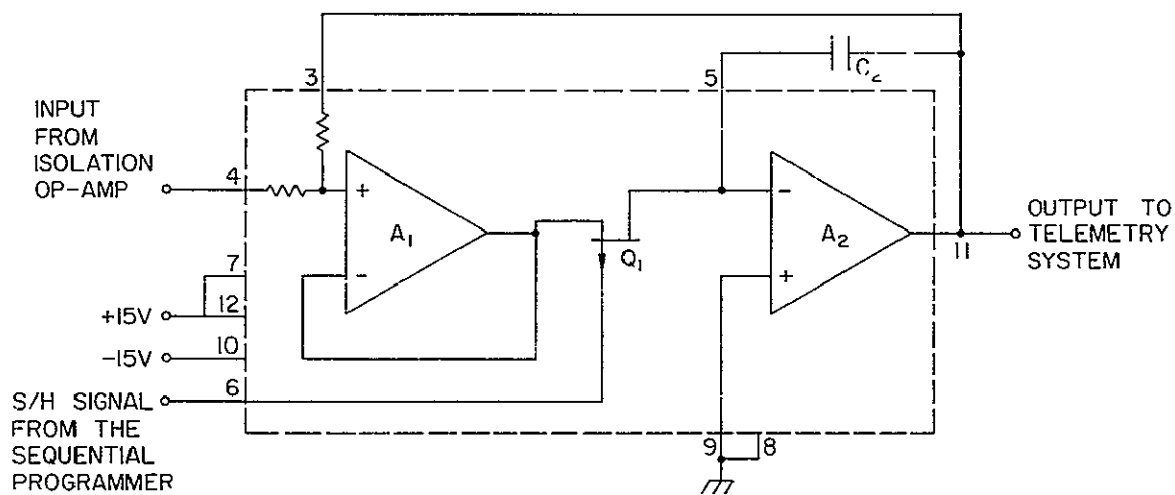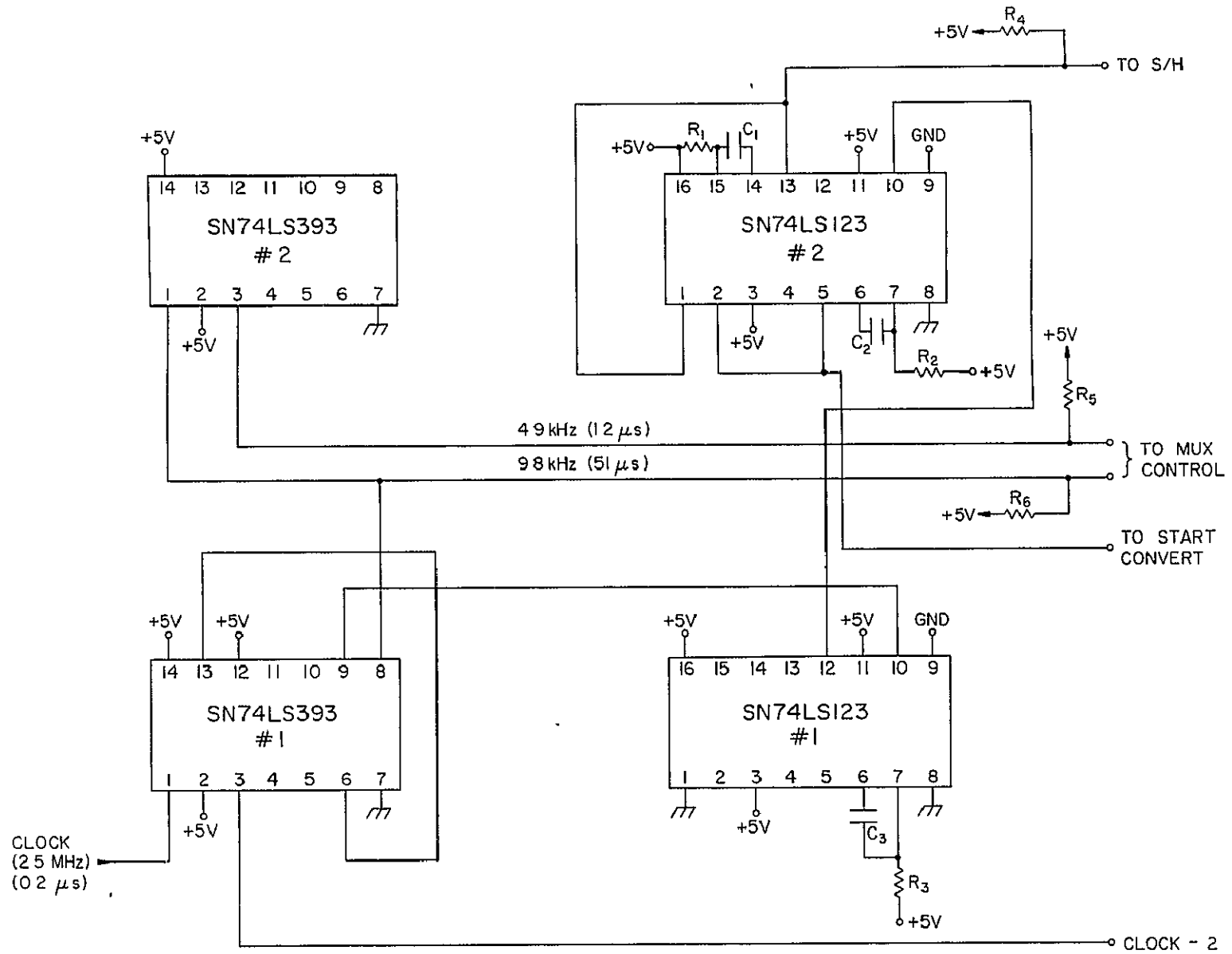Figure 5.11   Sample-and-hold circuit in the PHA using the LH0053C.

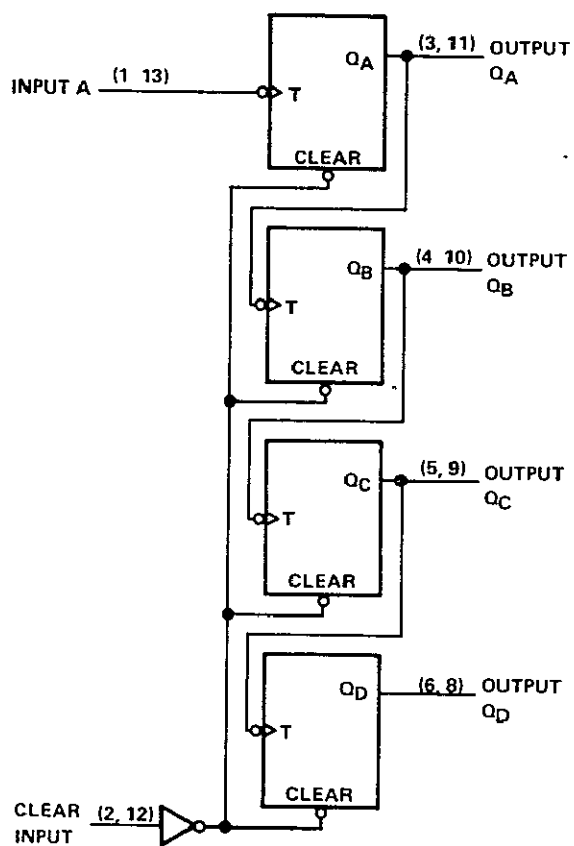Figure 5.12 The sequential programmer.

55

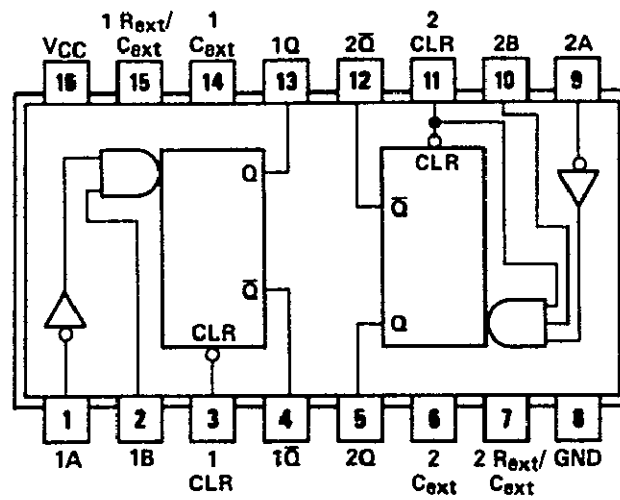Figure 5.13   Block schematic of the SN74LS393.

Figure 5.14 Block schematic and pin configuration of the SN74LS123.

pulse width of the start-convert signal is required to be greater than 2.4 μs in order to trigger the A/D converter properly. By adjusting the time constants of the one-shots, the desired start-convert signal, shown in Figure 5.15, is obtained. The time constants of the one-shots are controlled by the external capacitors and resistors (see Figure 5.14). The values of the components can be calculated using

$$t_w = k\ R_{ext}\ C_{ext}\ \left[1 + \frac{0.7}{R_{ext}}\right] \tag{5.5}$$

In the equation, t_w is the output pulse width (in ns), k has the value 0.33, R_{ext} is the external timing resistor (in kΩ) and C_{ext} is the external timing capacitor (in pF).

The sampling rate of the S/H is fixed to be one-fifth of the multiplexing rate. By feeding back the output of the one-shot in SN74LS123 #2 to the inverting input terminal, the S/H control signal shown in Figure 5.16 is obtained. The signal gives a sampling time of 10 μs and a holding time of 240 μs.

Figure 5.15 shows all the control signals and some important intermediate waveforms upon which the control signals are based.

5.8 *The Magnetometer-Signal Analyzer*

The circuit of the magnetometer-signal analyzer, as shown in Figure 5.16, is composed of two comparators (½MC3302P), a one-shot (½SN74LS123) and a binary counter (½SN74LS393). The electrical characteristics of the MC3302P resemble those of the LM239A, except that the LM239A has a faster response time.

The frequency of the magnetometer signal is about 7 Hz and each period of the signal is divided into discrete intervals of 10 ms duration (see Section 4.3). The digital information of these intervals is supplied by the binary counter which is triggered by the square wave generator formed by the comparator A_2 and the circuit elements R_1, R_2, R_3, R_4 and C_1. Therefore, the frequency of the square wave generator is required to be 100 Hz. This frequency is set by R_1, R_3 and C_1. R_6 and R_7 form a voltage divider which clamps V_B at 2.4 V. R_2 and R_5 protect the positive input of A_2 and A_1 from overloading. They also minimize the voltage variation, caused by A_1 and A_2, on B and hence minimize the interaction between A_1 and A_2. R_4 is the pull-up resistor of the output transistor in A_2. By fixing the value of R_1
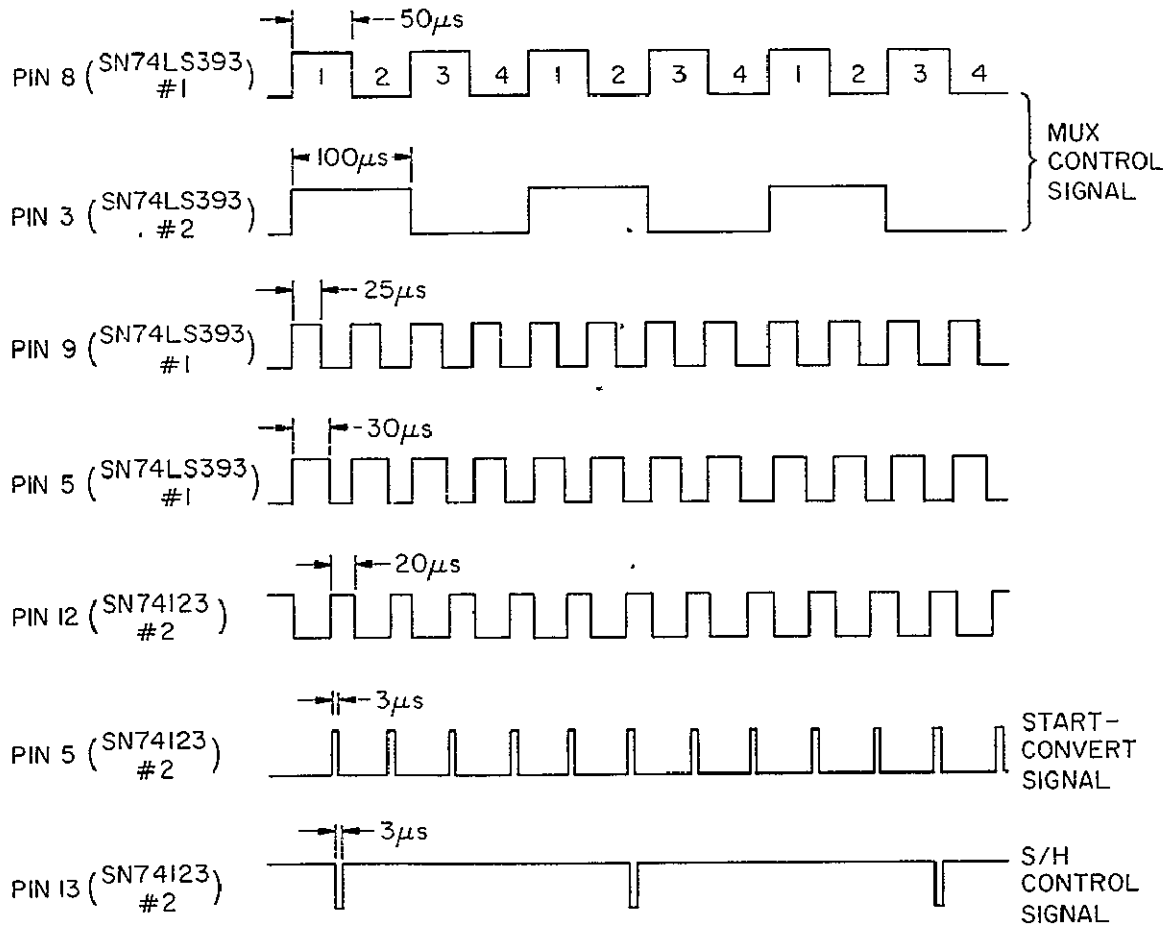
Figure 5.15 The output waveforms of the sequential programmer.
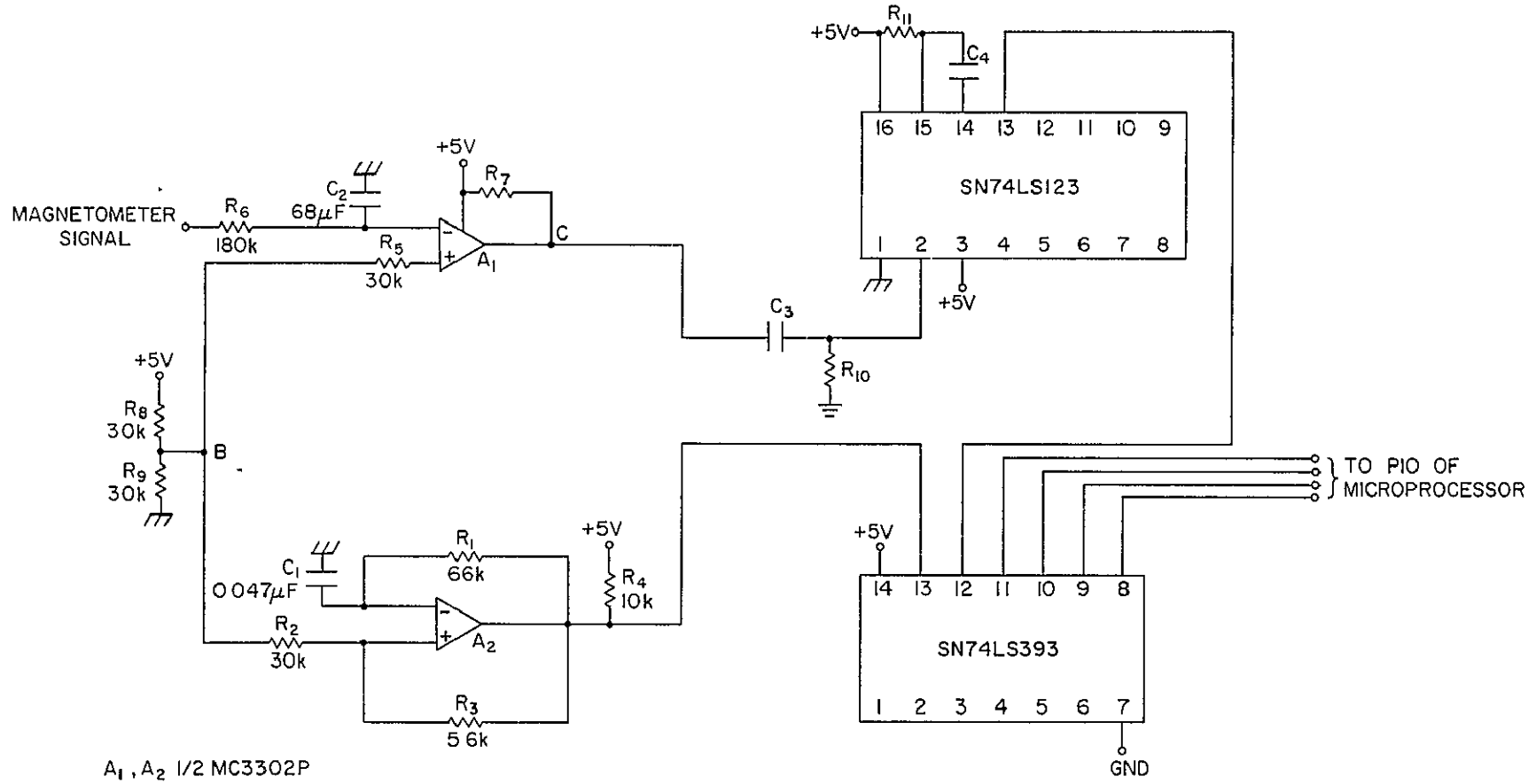
Figure 5.16 The circuit of magnetometer-signal analyzer.

and C_1 to be 5.6 kΩ and 0.047 µF, the value of R_1 can be calculated by using the circuit in Figure 5.17. As shown in the diagram, the voltage at the positive terminal of A_2 is given by:

$$V_+ = \frac{R_2}{R_2+R_3+R_4} \times V_{CC} \quad \frac{R_3+R_4}{R_2+R_3+R_5} \times V_B \tag{5.6}$$

$$V_+ = \frac{30k}{30k+5.6k+10k} \times 5 + \frac{4.6k+10k}{30k+5.6k+10k} \times 2.5 = 4.2 \text{ V}$$

The output of A_2 is

$$V_o = \frac{R_4}{R_2+R_3+R_4} \times V_B + \frac{R_2+R_3}{R_2+R_3+R_4} \times V_{CC} \tag{5.7}$$

$$V_o = \frac{30k}{30k+5.6k+10k} \times 2.5 + \frac{30k+5.6k}{30k+5.6k+10k} \times 5 = 4.45 \text{ V}$$

With these results R_1 can be calculated using

$$V_+ = V_o \left[1 - \exp\left(- \frac{T}{(R_1+R)C_1} \right) \right] \tag{5.8}$$

where T is the period of the square wave and $T = 1/f = 0.01$ s; R is the Thevenin equivalent resistor; $R_2 = R_4 || (R_2+R_3) = 7.8$ kΩ; and $C_1 = 0.047$ µF. The value of R_1 is calculated to be 66 kΩ.

The binary counter triggered by the square wave is reset at an interval equal to the period of the magnetometer signal. The reset pulse is generated by the one-shot. The reset-pulse width is 3 µs which is determined by C_4 and R_9 and equation (5.4). The one-shot is triggered by the zero-crossing detector formed by A_1, R_6, R_7, R_8, C_2 and C_3. R_6 and C_2 forms a low-pass filter to remove higher harmonics and noise from the magnetometer signal. Since the magnetometer output is biassed by 2.4 V, the reference voltage at the positive terminal of A_2 is, therefore, also set at 2.4 V. The output of A_2 latches on high (5 V) when the input sine wave is on the lower cycle (less than 2.4 V) and low (0 V) on the upper cycle (greater than 2.5 V). R_3 and C_3 form a differentiator so that only the changes in the output voltage of A_2 has effect on the input terminal (pin 2) of the one-shot. Since the TTL one-shot is triggered only by the rising edge of a positive pulse and this positive pulse occurs only once in every cycle of the magnetometer signal, therefore, a reset pulse is generated by the one-shot in every
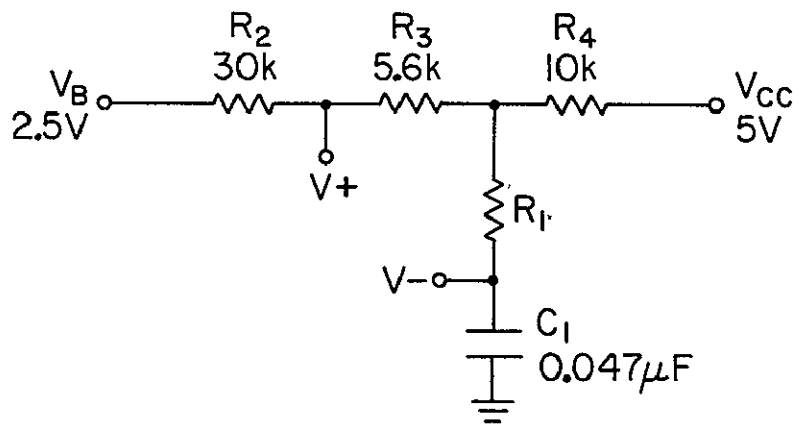
Figure 5.17 Equivalent circuit of the square-wave
generator used to calculate R_1.

period of the magnetometer signal. The output waveforms of the zero-crossing detector and the one-shot are shown in Figure 5.18.

The four outputs of the counter are interfaced to the microprocessor through the parallel input-output logic array (PIO).

5.9 *The Power Supply and the Finished System*

Three power supplies are required in the system: ±15 V and +5 V. The ±15 V supplies are sources for the analog circuits, which include the peak detectors, the multiplexers, the AM462 op-amps and the S/H. The noise in the power supplies of the analog circuits introduces error to the data processed. In order to minimize this error 0.1 μF capacitors are connected to the power supply pins of each analog-integrated chip. This minimizes both the power supply noise passing into the chip and the data signal coupling into the power supply. The +5 V supply is the source for the digital circuits. Noise with frequencies equal to the switching rates of the digital circuits is usually introduced into the power supply and this noise is introduced back to the circuits. As a result, the output waveforms of the digital circuits contain noise and ringing. Pull-up resistors are used to counteract this, especially for the circuits which generate the analog-circuit-control signals.

A picture of the complete pulse-height analyzer is shown in Figure 5.19. The complete data processing system, including the power supply circuits (lowest deck), the pulse-height analyzer (second lower deck) and the microprocessor (upper three decks), is shown in Figure 5.20.
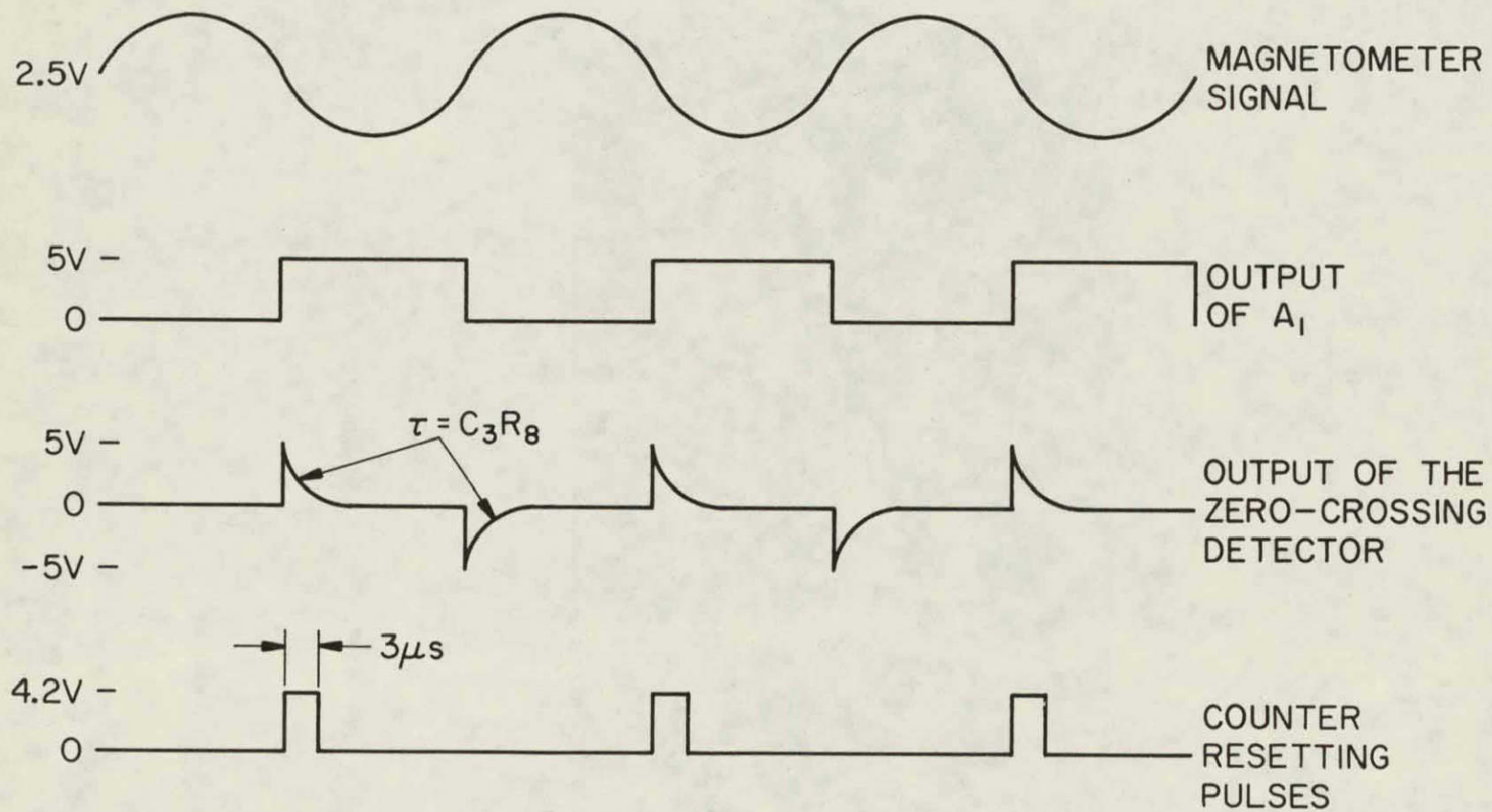
Figure 5.18 The output waveforms of the zero-crossing detector and the one-shot.
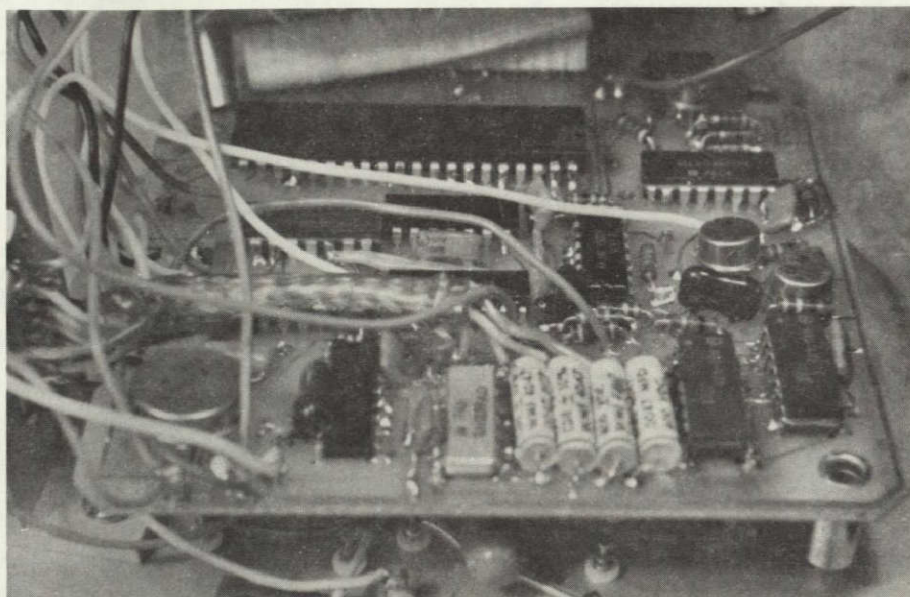
Figure 5.19 The pulse-height analyzer.
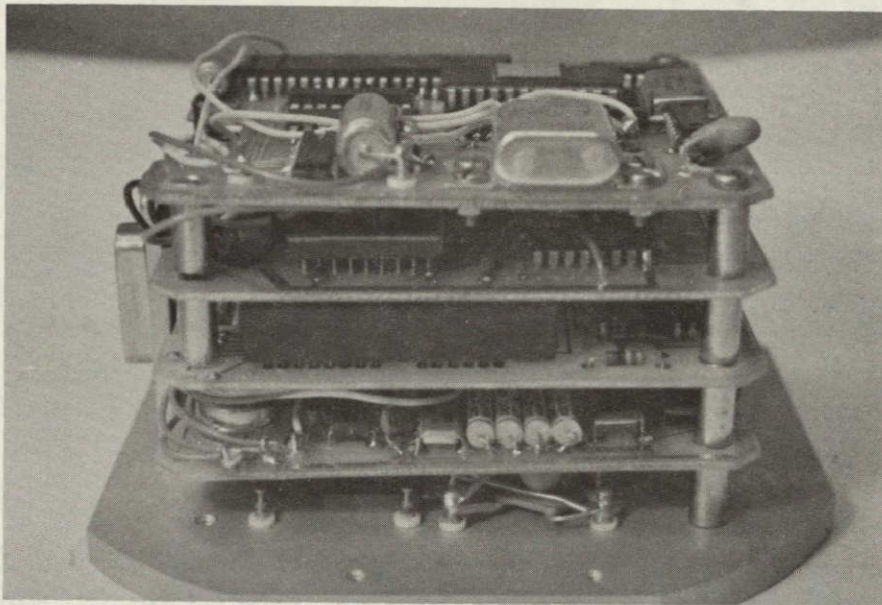
Figure 5.20 The complete data processing system.

6. PRELIMINARY RESULTS AND METHODS FOR DATA REDUCTION

Nike Apache 14.543 was launched at 2315 EST on 19 June 1978 from Wallops Island, Virginia. Data received through the telemetry system are obtained both as analog and digital tapes. Some of the preliminary results obtained from the analog tape are discussed in Section 6.1. Methods for data reduction using both analog and digital tapes are described in Section 6.2.

6.1 *Preliminary Results Obtained from the Analog Tape*

A portion of a chart record obtained from the analog tape of Nike Apache 14.543 is shown in Figure 6.1. Telemetry channel H records the output data from the S/H. Channel 18 records data from the output of the microprocessor. Channel 6 records the output of the spin magnetometer. The other six channels on this record show the outputs of the counting circuits. [For more information on the counting electronics, see *Voss and Smith*, 1974]. It will be shown in the next section that the data obtained from the counting circuits are very helpful for the data reduction of the S/H channel. The waveform recorded at the top of the chart represents the coded time.

The data on channel H are shown inverted in Figure 6.1. Each pulse has a width of 250 µs. The amplitude of the pulse provides information on the energy level of the energetic particle detected. Figure 6.2 shows signal waveforms of channel H of the analog tape of Nike Apache 14.5-3. Since the telemetry channel does not have infinite bandwidth, the pulse waveform of the S/H output is distorted during the transmission process. By passing the recorded signal through a low-pass filter, most of the transmission noise is removed and the waveform is smoothed. Figures 6.2(a) and (b) are obtained by passing the analog signal from the tape through a 6 kHz low-pass filter. Figure 6.2(c) is obtained from the output of an 8 kHz filter.

The figures show the difference of using different low-pass filters: the lower the cut-off frequency of the filter used, the smoother is the resulting waveform. However, using a lower cut-off frequency filter will also increase the rise and fall time of the pulses. The distortion of the waveform can be noticed by comparing these graphs with those in Figures 5.9 and 5.10.

The results shown in Figures 6.1 and 6.2 confirm that the design of the PHA is successful. Figure 6.2 further shows that the crosstalk between the four channels is negligible.

Figure 6.1   Section of chart record from Nike Apache 14.543.   The
output of the multiplexer is on channel H and of the
microprocessor is on channel 18.   Circles have been
drawn around the larger isolated pulses from the
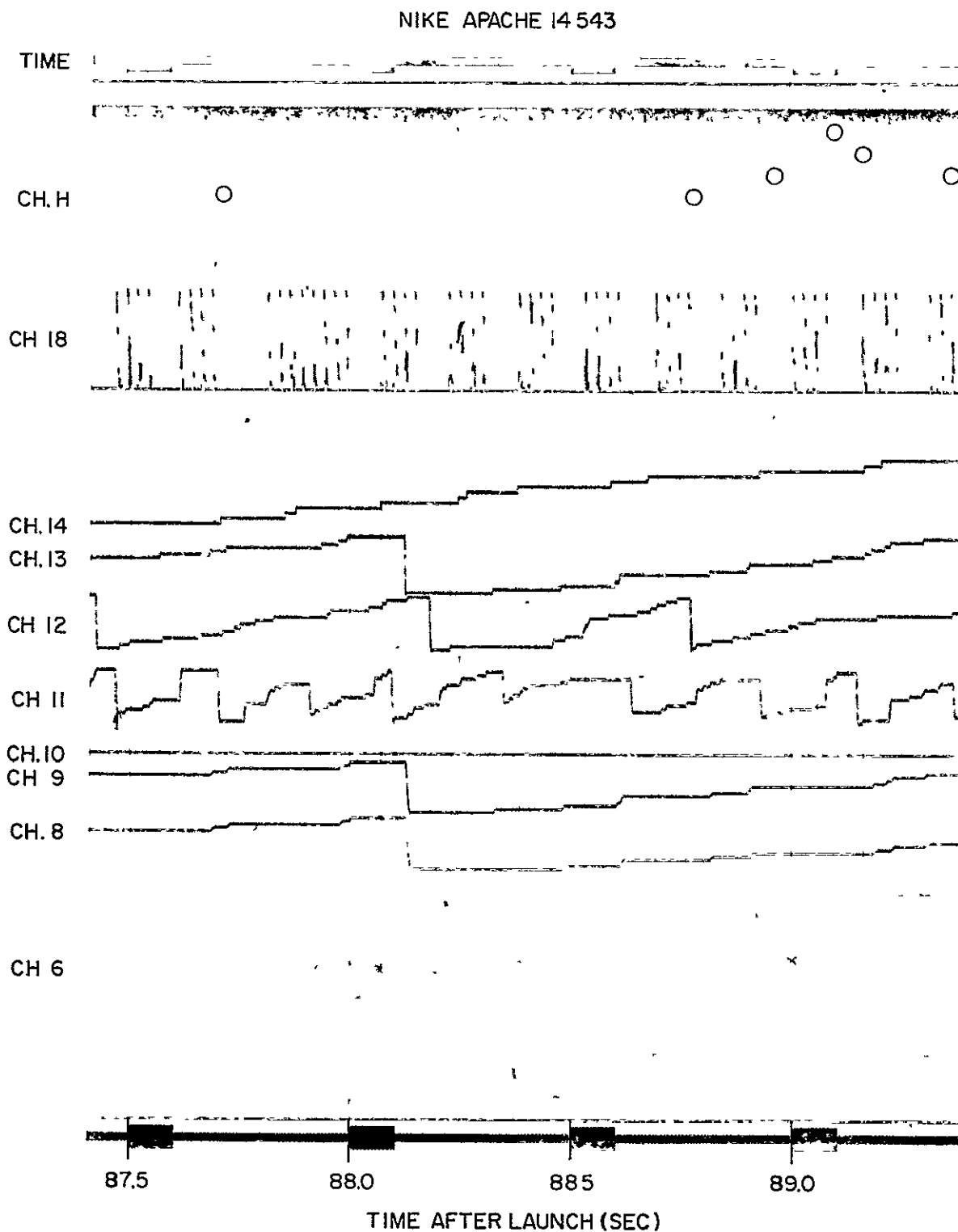multiplexer.
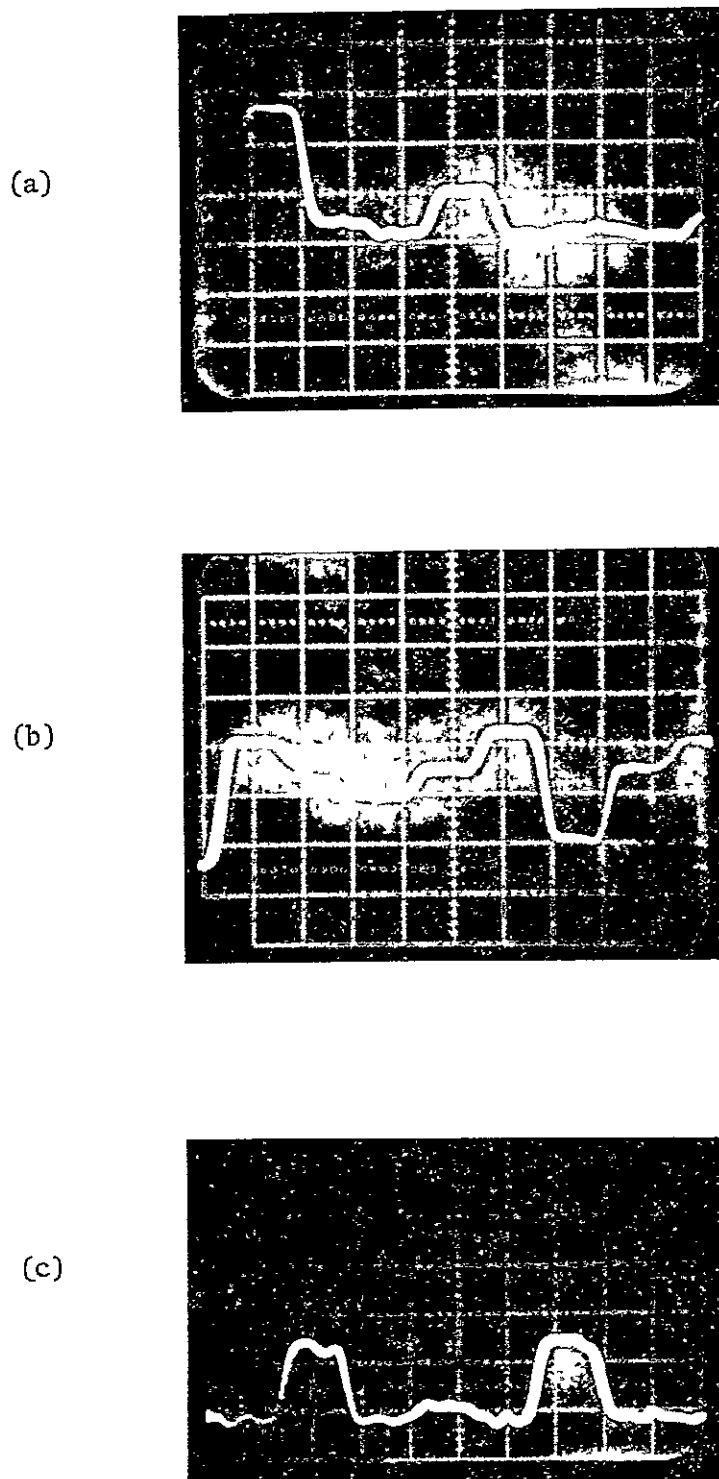
Figure 6.2 S/H output waveform obtained from the analog tape
of Nike Apache 14.543. The output filter for (a)
and (b) is 6 kHz; for (c) it is 8 kHz.

6.2 *Methods for Data Reduction*

The term data reduction is interpreted here as the process of sorting out the data available in the tapes from the noise and putting them into groups so that the relations between one group and the other can be obtained easily.

The data transmitted from the rocket to the ground station are recorded in both digital and analog data tapes. Therefore, data reduction can be done by using either analog or digital data tapes. In the following subsections, data-reduction methods using both types of data tapes are suggested and discussed.

6.2.1 *Data-reduction systems using analog data tapes.* After the reduction processes described below the data will be either sorted into arrays or used in obtaining graphs. The data arrays provide the following information on a particle detected: the energy (represented by pulse height), the time at which the particle is detected and the pitch angle.

The system shown in Figure 6.3 can be used for data reduction. Data from several channels are recorded in one chart (see Figure 6.1). Only the magnetometer channel, the S/H channel and the coded time channel are useful in the process. The analog data from the tape are frequency modulated, therefore, frequency discriminators are needed to recover the data. These discriminators are provided with tape speed compensation. Low-pass filters in the system are used to filter out transmission noise.

During the operation of the system the encoded-time signal, after passing through the frequency discriminator and the low-pass filter, is decoded by the time-code translator. The recovered digital time signal is then used to synchronize the digitizing process of the other two channels. The frequency demodulated analog data of the S/H and the magnetometer are digitized by analog-to-digital converters (A/D). The converters are controlled by the time synchronization circuit. The digital data of the S/H, the magnetometer and the time of the rocket flight are then interfaced to a minicomputer.

The output data rate of the A/D converters are required to be high in order to make an optimal use of the analog data available. However, the output device of a digital computer such as a printer usually has a low output rate. Therefore, one main function of the computer is to adapt its input data rate to its output data rate. Data manipulation can also be done inside the minicomputer. The output of the minicomputer may be used either to drive a plotter so that data profiles can be obtained directly or to
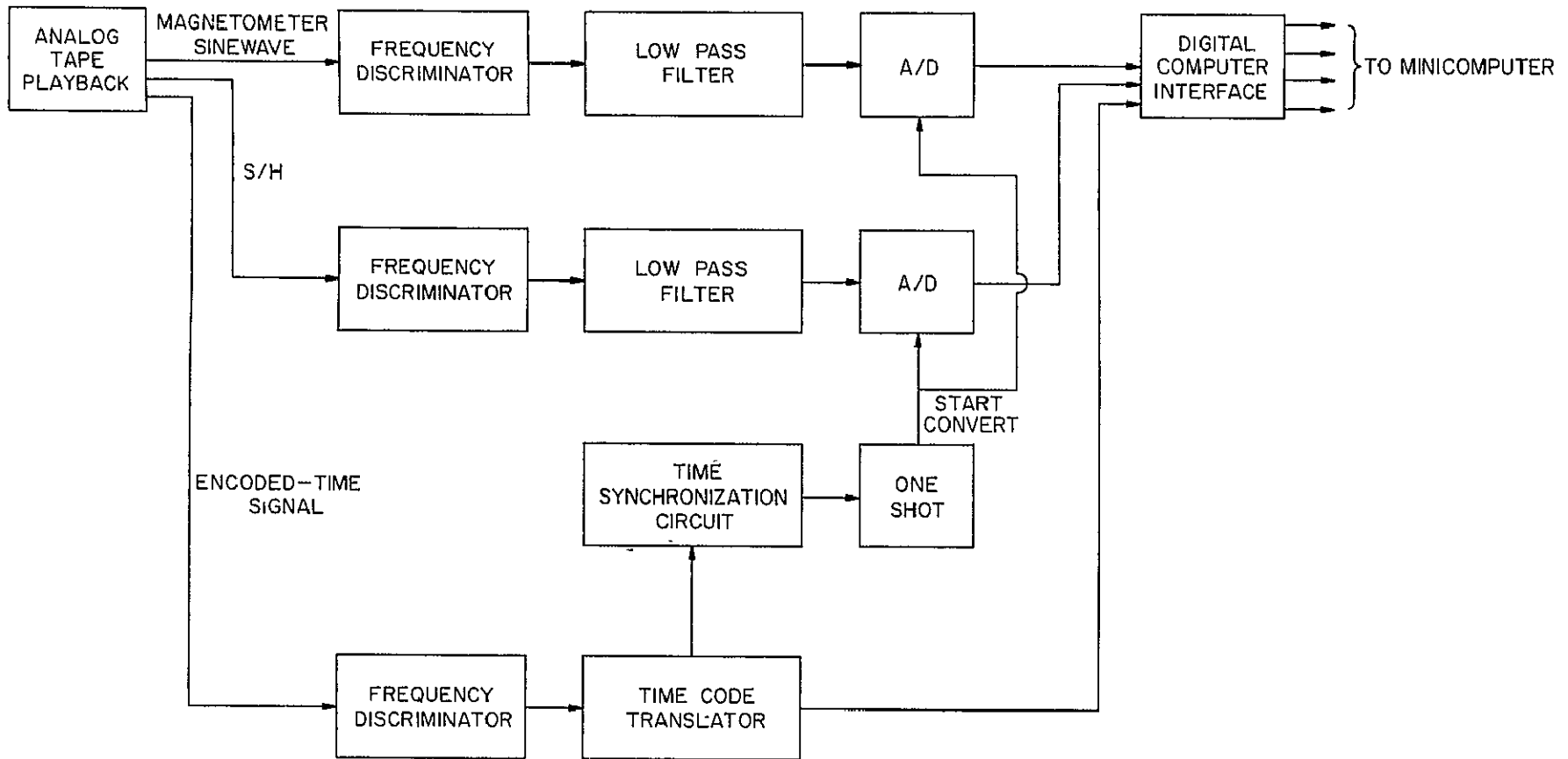
Figure 6.3   Data-reduction system using an analog data tape.

control a printer.

The time-controlled digitizing process can, with advantage, be changed to the data-controlled digitizing process. The chart record in Figure 6.1 shows that the crosstalk between the input channels of the PHA is negligible and that the probability of two pulses appearing at the same time at the inputs of two adjacent channels is close to zero. Therefore, the pulses of the S/H can be used to control the A/D converters. This is accomplished by replacing the time synchronization circuit with the circuit shown in Figure 6.4.

In Figure 6.4 V_{REF} is set equal to the noise level of the S/H channel. When a pulse occurs at the positive terminal of the comparator, the output of the comparator changes states and triggers the one-shot. The one-shot sends out a pulse to the start-convert input of the A/D converters and activates the digitizing process.

Since the data-control digitizing process records data only when a pulse occurs and since the data rate of the S/H is low (see the chart record in Figure 6.1), much irrelevant data obtained in the time-control process are eliminated.

The data-reduction systems described in this section are very powerful. They speed up the data-reduction process; they also save computer costs. The only problem with these processes is the development of a minicomputer system. However, once the system is developed, it can be used for most of the data-reduction of future rocket experiments.

6.2.2 *Data reduction using digital tape.* The output of the S/H consists of data from four different input channels. One problem of the data reduction described below is to identify the input channel from which a pulse is transmitted; the other problem is to find the pitch angle of the particle.

Inside the rocket payload the four data inputs of the PHA are also connected to the inputs of four independent counting circuits. The output of these are staircase waveforms (see Figure 6.1). Each staircase contains sixteen steps and each step represents the occurrence of a pulse. Whenever a pulse is recorded at the S/H output, the counting circuit of the corresponding input channel will also record a pulse by showing a jump in its output waveform. The input channel from which the pulse is transmitted can therefore be identified.
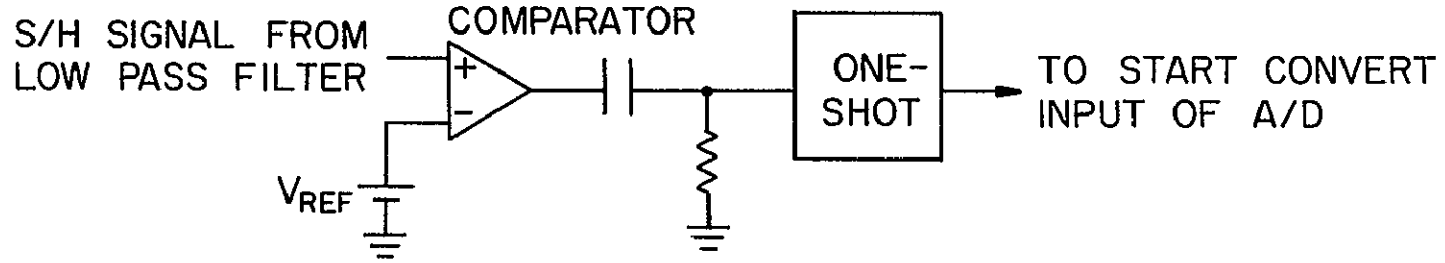
Figure 6.4   Data-controlled synchronization circuit.

7. CONCLUSIONS AND SUGGESTIONS FOR FUTURE WORK

7.1 *Conclusions*

The design of the PHA basically is successful. The system in Nike Apache 14.543 performed satisfactorily throughout the whole rocket flight. The data sent back through the microprocessor output channel shown in Figure 6.1 show the successful performance of the PHA in data acquisition.

The data obtained from the S/H channel are surprisingly useful because they have a better amplitude resolution than those obtained from the micro-processor and the counting circuits. The data obtained from the microprocessor, however, are already essentially complete and needs only a very simple data-reduction program. Therefore, the purpose of this data-manipulation experiment in simplifying the data-reduction process has been achieved.

7.2 *Suggestions for Future Work*

The performance of the pulse-height analyzer as a whole can be improved. The improvements of individual stages by using different circuit elements are first discussed. The system can also be improved through the replacement of several building blocks by commercially available integrated chips. Finally, an alternative design for the PHA is described.

7.2.1 *The peak detector.* The peak detector described in Chapter 5 can accurately detect pulses having an amplitude between -1 and -7.5 V and a rise time of 1.5 µs. However, in order to optimize the performance of the pre-amp and shaper, the peak detector is required to detect-accurately pulses of amplitude from 0 to -10 V and of 1 µs rise time. This can be achieved by using comparators of higher slew rates such as the LM219, which has a response time of 80 ns compared to the 1.3 µs of the LM239A. The LM219 is a dual comparator and is available in 10-pin metal cans, therefore, two of them together should only occupy a little more circuit space than an LM239A.

7.2.2 *The log-amp.* The 8048 log-amp was finally abandoned because of the difficulties in obtaining a suitable settling time. A faster log-amp can be constructed by using two high slew rate op-amps (such as the µA715). A thermistor can be used in the circuit for temperature compensation. However, a fast log-amp always has a stability problem. A digital logarithmic converter is fast and does not have a stability problem. The converter can be realized by using a programmable read-only memory (PROM) serving as a look-up table. The PROM is available commercially or it can be programmed

by a microprocessor. The PROM must be inserted following the A/D converter in the system since it only takes digital input signals.

7.2.3 *The sample-and-hold circuit.* Data reduction is simplified if a synchronization pulse is generated at the output of the S/H and included with the data. The synchronization pulse serves as a reference, so that the channel from which a piece of data originates can be easily identified.

Figure 7.1 shows the circuit of an S/H that can generate synchronization pulses. The circuit makes use of the other JFET (gate 2) inside the LH0053C. Gate 2 is controlled by the pulses generated by a one-shot which is triggered by the output of the binary counter. The counter counts only when both of the multiplexing control signals go low (i.e., when channel 1 is turned on). When the counter registered $2^7 = 128$ counts, the one-shot is triggered and the counters are, at the same time, reset. The control pulse generated by the one-shot closes the JFET switch and the -5 V appears at the negative input terminal of A_2, then the output voltage of the integrator formed by A_2 and C will change at $-5 \times 1/(R+R_s)C$ V s^{-1}, where R_s represents the on-channel impedance of the JFET. The integration time is determined by the pulse width of the control pulse which is set by R_{ext} and C_{ext} in equation (5.5). Such an output waveform would appear every $50 \times 10^{-6} \times 4 \times 128 = 25.6$ ms during the rocket flight and its presence would indicate that channel one is switched on at that particular time.

7.2.4 *The main conversion channel as an integrated chip.* The complete conversion channel including the multiplexer, inverter, isolation op-amp and the A/D converter can be replaced by a recently available integrated chip such as the MN7100. It is a 32-pin DIP with a throughput rate of 90,000 conversions per second. By using an MN7100 the size of the PHA can be reduced by a factor of 2. The block diagram representing the MN7100 is shown in Figure 7.2. The connections of the MN7100 with the other components in the PHA are also indicated in the diagram.

7.2.5 *Design of the PHA using voltage-to-frequency conversion technique.* The PHA shown in Figure 7.3 makes use of the low cost monolithic voltage-to-frequency converter (V/F) [*Morrison,* 1978]. The pulse-height signal at the output of a peak detector is converted by the V/F to a pulse train with the period of the output pulses directly proportional to the height of the input pulses. The pulse train is then used to modulate the pulses generated by the gate oscillator. The number of pulses registered in the counters represents
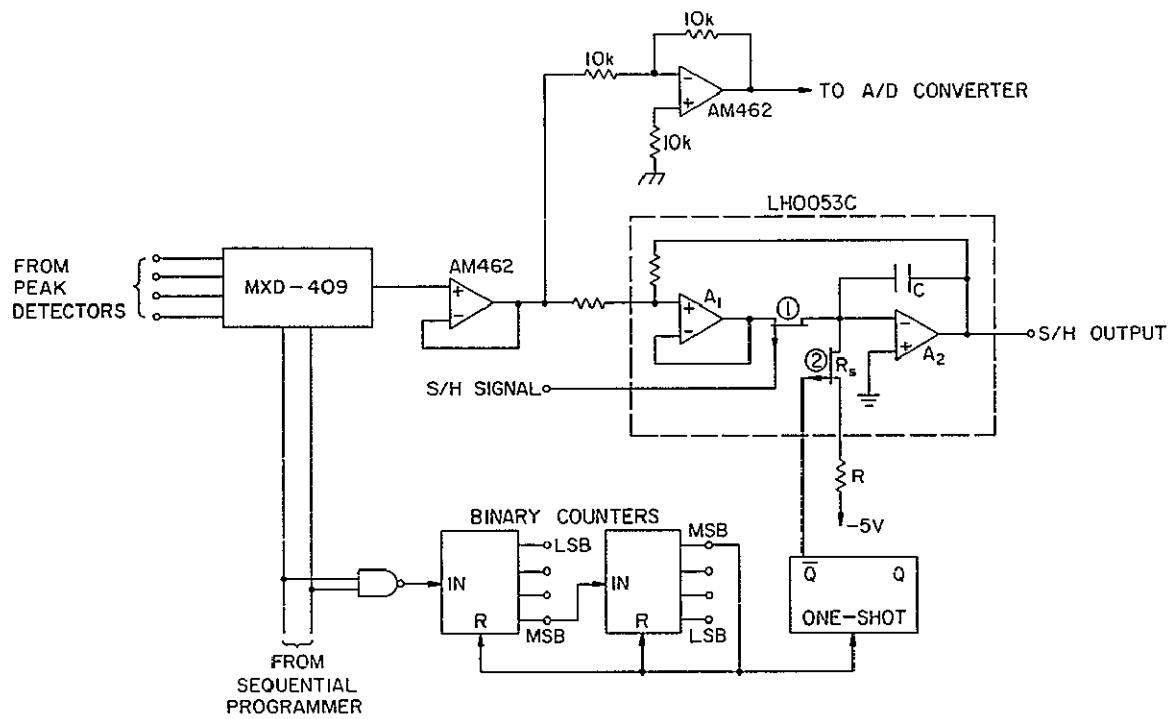
Figure 7.1   A sample-and-hold circuit that generates synchronization
pulses.
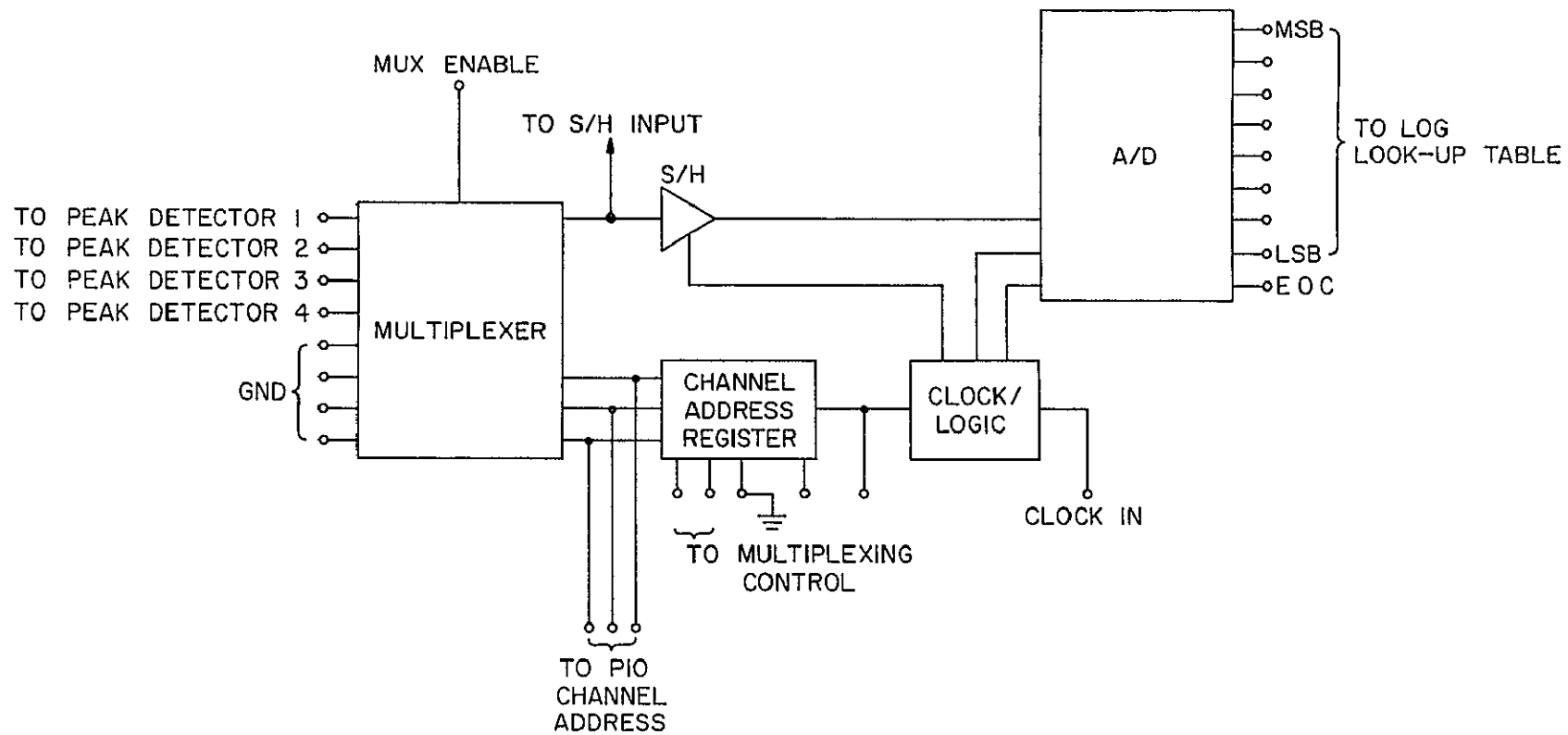
Figure 7.2 The block diagram of the MN7100 data-acquisition system.
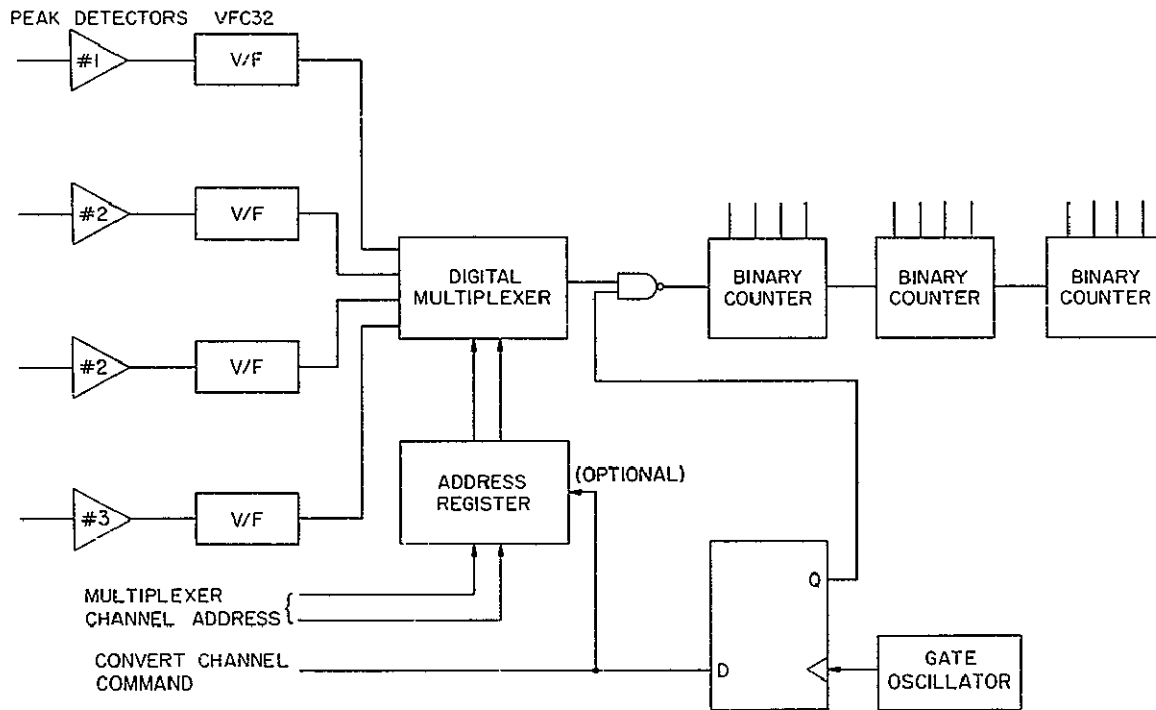
Figure 7.3 A data-acquisition system using the voltage-to-frequency conversion technique [*Morrison*, 1978].

a parallel digital code of the height of the output pulse from the peak detector. The frequency of the gate oscillator and the conversion period determines the resolution of the output data. Both the conversion control signal and the multiplexer-channel-address signals can be controlled by the sequential programmer or directly by a microprocessor.

The PHA using the V/F conversion technique provides high noise immunity and eliminates the conversion errors encountered in the PHA when using the classical design technique described in Chapter 4.

REFERENCES

Cornwall, J. M. [1971], Transport and loss processes for magnetospheric helium, *J. Geophys. Res., 76,* 264-267.

Davis, L. L., L. G. Smith, and H. D. Voss [1979], A rocket-borne data-manipulation experiment using a microprocessor, *Aeron. Rep. No. 84,* Aeron. Lab., Dep. Elec. Eng., Univ. Ill., Urbana.

Hayakawa, S. T. Kato, T. Kohno, T. Murakami, F. Nagase, K. Nishimura, and Y. Tanaka [1973], Existence of geomagnetically trapped electrons at altitudes below the inner radiation belt, *J. Geophys. Res., 78,* 2341-2343.

Hill, R. W., R. J. Grader, F. D. Seward, and J. P. Stoering [1970], Soft particle flux above 130 km at midlatitude, *J. Geophys. Res., 75,* 7267-7271.

Moritz, J. [1972], Energetic protons at low L-values of the equatorial magnetosphere, *Space Res., XIII,* Akademie-Verlag, Berlin, 669-674.

Morrison, R. L. [1978], Microcomputers invade the linear world, *IEEE Spectrum, 15,* 38-41.

Ogawa, T and T. Tohmatsu [1966], Photoelectronic processes in the upper atmosphere, II. The hydrogen and helium ultraviolet glow as an origin of the nighttime ionosphere, *Rep. Ionospheric Space Res., Japan, 20,* 375-417.

Pozzi, M. A., L. G. Smith, and H. D. Voss [1979], A rocket-borne electrostatic analyzer for measurement of energetic particle flux, *Aeron. Rep. No. 82,* Aeron. Lab., Dep. Elec. Eng., Univ. Ill., Urbana.

Shen, J. S., W. E. Swartz, D. T. Farley, and R. M. Harper [1976], Ionization layers in the nighttime E-region valley above Arecibo, *J. Geophys. Res., 81,* 5517-5526.

Strobel, D. F., T. R. Young, R. R. Meier, T. P. Coffey, and A. W. Ali [1974], The nighttime lower ionosphere, *J. Geophys. Res., 79,* 3171-3178.

Voss, H. D. and L. G. Smith [1974], Design and calibration of a rocket-borne electron spectrometer for investigation of particle ionization in the nighttime midlatitude E region, *Aeron. Rep. No. 62,* Aeron. Lab., Dep. Elec. Eng., Univ. Ill., Urbana.

Voss, H. D. and L. G. Smith [1977], Energetic particles and ionization in the nighttime middle and low ionosphere, *Aeron. Rep. No. 78,* Aeron. Lab., Dep. Elec. Eng., Univ Ill., Urbana.

Voss, H. D. and L. G. Smith [1979], Nighttime ionization by energetic particles at Wallops Island in the altitude region 120 to 200 km, *Geophys. Res. Lett.*, *6*, 93-96.

APPENDIX I.   Program for Reading Digital Tapes

The program listed below is written by W. Knecht and modified by H. D. Voss for the data reduction of rocket experiments.

The program reads data from a digital tape and sorts the data into arrays. Further data manipulation can be done by using these data arrays. The program also uses the data arrays obtained from the counting circuit channels and calculates the number of particles detected per second during the rocket flight.

```
FORTRAN IV G LEVEL 21          MAIN          DATE = 77270          13/20/20
          C     PROGRAM EEDPROC
          C     READS WALLOPS DIGITAL TAPES AND FORMATS EED DATA SAMPLES FOR
          C     ANALYSIS BY SUBROUTINES
0001            INTEGER*4 TIMPRT,RECHRS,RECMIN,EEDCH1,EEDCH2,EEDCH3,EEDCH4,
                EEDCH5,
                1CURHRS,CURMIN,HRS,FSTSEC,DATAID(20)
0002            INTEGER*2 ARRAY(2008),EED1(1000),EED2(1000),EED3(1000),
                EED4(1000),
                1EED5(1000),COUNT1(400),COUNT2(400),COUNT3(400),COUNT4(400),
                1COUNT5(400)
0003            DOUBLE PRECISION RECTIM,ENDREC,ENDNEX,CVITIM,INITIM
0004            DOUBLE PRECISION STARTM,ENDTIM,CURTIM,LCHTIM
0005            REAL*4 ITINCR
0006            COMMON ARRAY,TIMPRT,NUMREC,NUMHED,NUMCAL,RECHRS,RECMIN,RECSEC
0007            NAMELIST/PARMS/NUMHED,NUMCAL,ICHECK
0008            NAMELIST/CHANS/EEDCH1,EEDCH2,EEDCH3,EEDCH4,EEDCH5
0009            NAMELIST/TIMES/FSTSEC,LSTSEC
0010            CVTTIM(HRS,MINS,SECS)=3.6D3*HRS+6.D1*MINS+1.D0*SECS
0011            READ (5,PARMS)
0012            READ (5,TIMES)
0013            READ (5,CHANS)
0014            READ (5,801) LCHRS,LCHMIN,LCHSEC
0015        801 FORMAT (2I2,1X,I2)
0016            READ (5,802) DATAID
0017        802 FORMAT (20A4)
0018            WRITE (11,807)
0019            WRITE (6,807)
0020        807 FORMAT (1H1)
0021            WRITE (11,PARMS)
0022           -WRITE (11,TIMES)
0023            WRITE (11,CHANS)
0024            WRITE (6,804) DATAID
0025        804 FORMAT (1X,20A4)
0026            WRITE (6,803) LCHRS,LCHMIN,LCHSEC
0027        803 FORMAT (1X,'LAUNCH TIME:   ',2I2,':',I2)
0028            IWRITE=0
0029            NUMREC=0
0030            TIMPRT=1
0031            READ (5,489) ICMAX,ICMIN
0032        489 FORMAT (2I6)
```

```
0033            WRITE (6,486) ICMAX,ICMIN
0034        486 FORMAT (/,1X,2I6)
0035            IDELCO=(ICMAX-ICMIN)/16
0036            K=1
0037            DO 589 J=1,400
0038            COUNT1(J)=0
0039            COUNT2(J)=0
0040            COUNT3(J)=0
0041            COUNT4(J)=0
0042        589 COUNT5(J)=0
0043            CALL TPREAD
        C   CALCULATE TIME OF FIRST DATA SAMPLE NEEDED
0044            RICSEC=LCHSEC
0045            LCHTIM=CVTTIM(LCHRS,LCHMIN,RLCSEC)
0046            WRITE (11,850) LCHTIM
0047        850 FORMAT (1X,'LAUNCH TIME CONVERTED TO SECONDS:  ',F9.2/)
0048            STARTM=LCHTIM+FSTSEC          .
0049            ENDTIM=LCHTIM+LSTSEC
0050            CURTIM=STARTM
0051            INITIM=STARTM
        C   LOCATE RECORD CONTAINING FIRST SAMPLE NEEDED
0052        130 CALL DAREAD (IWRITE)
0053            RECTIM=OVTTIM(RECHRS,RECMIN,RECSEC)
0054            IF(ICHECK.GE.1) WRITE (11,813) RECTIM
0055        813 FORMAT ('+',50X,'RECTIM=  ',F12.5)
0056            ENDREC=RECTIM + 0.3998D0
0057            IF (RECTIM-INITIM) 133,133,132
0058        132 WRITE (11,812)
0059        812 FORMAT (1X,'START TIME IS EARLIER THAN TIME OF FIRST RECORD')
0060            STOP 5
0061        133 IF (INITIM.LE.ENDREC) GO TO 135
0062            ENDNEX=RECTIM + 0.7998D0
0063            IF (INITIM.LE.ENDNEX.AND.ICHECK.GE.2) IWRITE=1
0064            GO TO 130
        C   DETERMINE SUBSCRIPT OF FIRST DATA SAMPLES NEEDED
0065        135 ITINCR=INITIM-RECTIM
0066            INDEX=5000.*ITINCR+6.
0067            IDXFST=5+5*((INDEX-1)/5
0068            IF (IDXFST.LT.2005) GO TO 136
0069            CALL DAREAD (IWRITE)
0070            RECTIM=CVTTIM(RECHRS,RECMIN,RECSEC)
0071            IDXFST=5
        C   DETERMINE SUBSCRIPTS OF FIRST SAMPLES FOR EACH CHANNEL
0072        136 IDXCH1 = IDXFST + EEDCH1
0073            IDXCH2 = IDXFST + EEDCH2
0074            IDSCH3 = IDXFST + EEDCH3
0075            IDXCH4 = IDXFST + EEDCH4
0076           .IDXCH5 = IDXFST + EEDCH5
0077            IF(ICHECK.GE.1) WRITE(11,805) INDEX,IDXFST,IDXCH1,IDXCH2,
                IDXCH3,
               1IDXCH4,IDXCH5,NUMREC
0078        805 FORMAT (1X,'INDEX=',I4,3X,'IDXFST=',I4,3X,'IDXCH1=',I4,3X,
               1'IDXCH2=
```

```
                1',I4,3X,'IDXCH3=',I4,3X,'IDXCH4='I4,3X,'IDXCH5=',I4,3X,
                2'FIRST RECORD NUMBER= ',I4)
0079            IWRITE=0
0080            I=1
0081        137 EED1(I) = ARRAY(IDXCH1)·
0082            EED2(I) = ARRAY(IDXCH2)
0083            EED3(I) = ARRAY(IDXCH3)
0084            EED4(I) = ARRAY(IDXCH4)
0085            EED5(I) = ARRAY(IDXCH5)
0086            IDXCH1 = IDXCH1 + 5
0087            IF(IDXCH1.GT.2005) GO TO 140
0088            IDXCH2=IDXCH2+5
0089            IDXCH3=IDXCH3+5
0090            IDXCH4=IDXCH4+5
0091            IDXCH5=IDXCH5+5
0092            GO TO 150
0093        140 CALL DAREAD (IWRITE)
0094            RECTIM=CVTTIM(RECHRS,RECMIN,RECSEC)
0095            IDXCH1=EEDCH1 + 5
0096            IDXCH2=EEDCH2 + 5
0097            IDXCH3=EEDCH3 + 5
0098            IDXCH4=EEDCH4 + 5
0099            IDXCH5=EEDCH5 + 5
0100        150 I = I + 1
0101            IF (I.LE.1000) GO TO 137
0102            IF (ICHECK.GE.1) WRITE (11,814) IDXCH1,IDXCH2,IDXCH3,IDXCH4,
                IDXCH5
                1,NUMREC
0103        814 FORMAT(1X,'END INDICES:  IDXCH1=',I4,3X,'IDXCH2=',I4,3X,'IDXCH3=',
                114,3X,'IDXCH4=',I4,3X,'IDXCH5=',I4,3X,'LAST RECORD NUMBER=',I4)
0104            IF (ICHECK.GE.2) WRITE (11,816) NUMREC
0105        816 FORMAT (//1X,'RECORD NUMBER: ',I4)
0106            IF (ICHECK.GE.2) WRITE (11,815) ARRAY
0107        815 FORMAT (/101(' ',20I6/))
0108            CALL UTIME.(CURTIM,THRS,TMINS,CURSEC)
0109            CURHRS=THRS
0110            CURMIN=TMINS
0111            IRAMPS=0
0112            I=0  .
0113    ·   500 I=I+1
0114            IF (I-999) 501,504,504
0115        501 IF((EED1(I)-EED1(I+1))-(3*IDELCO)) 500,500,502
0116        502 IRAMPS=IRAMPS+1
0117            I=I+2
0118            IF (I-999) 501,504,504
0119        504 COUNT1(K)=IRAMPS*16-(EED1(1)-ICMIN)/IDELCO+(EED1(1000)-ICMIN)/
                1IDELCO
0120            IRAMPS=0
0121            I=1
0122        505 KA=EED2(I)-EED2(I+1)
0123            KB=EED2(I)-EED2(I+2)
0124            IF (KA.GT. 6*IDELCO .OR.KB.GT. 7*IDELCO) GO TO 507
0125            I=I+1
```

```
0126            IF (I-998)505,510,510)
0127        507 IRAMPS=IRAMPS+1
0128            I=I+5
0129            IF (I-998) 505,510,510
0130        510 COUNT2(K)=IRAMPS*16-(EED2(1)-ICMIN}/IDELCO+(EED2(1000)-ICMIN)/
                1IDELCO
0131            IRAMPS=0
0132            I=1
0133        511 KA=EED3(I)-EED3(I+1)
0134            KB=EED3(I)-EED3(I+2)
0135            IF (KA.GT. 7*IDELCO .OR.KB.GT. 8*IDELCO) GO TO 512
0136            I=I+1
0137            IF (I-998) 511,515,515
0138        512 IRAMPS=IRAMPS+1
0139            I=I+10
0140            IF (I-998) 511,515,515
0141        515 COUNT3(K)=IRAMPS*16-(EED3(1)-ICMIN)/IDELCO+(EED3(1000)-ICMIN)/
                1IDELCO
0142            IRAMPS=0
0143            I=1
0144        516 KA=EED4(I)-EED4(I+1)
0145            KB=EED4(I)-EED4(I+2)
0146            IF (KA.GT. 7*IDELCO .OR.KB.GT. 8*IDELCO) GO TO 517
0147            I=I+1
0148            IF (I-998)516,520,520
0149        517 IRAMPS=IRAMPS+1
0150            I=I+30
0151            IF (I-998)516,520,520
0152        520 COUNT4(K)-IRAMPS*16-(EED4(1)-ICMIN)/IDELCO+(EED4(1000)-ICMIN)/
                1IDELCO
0153            IRAMPS=0'
0154            I=1
0155        521 KA=EED5(I)-EED5(I+1)
0156            KB=EED5(I)-EED5(I+2)
0157            IF (KA.GT. 8*IDELCO .OR.KB.GT. 9*IDELCO) GO TO 522
0158            I=I+1
0159            IF (I-998)521,525,525
0160        522 IRAMPS=IRAMPS+1
0161            I=I+200
0162            IF (I-998)521,525,525
0163        525 COUNT5(K)=IRAMPS*16-(EED5(1)-ICMIN)/IDELCO+(EED5(1000)-ICMIN)/
                1IDELCO
0164            CURTIM=CURTIM+1.DO
0165            IF (CURTIM.GT.ENDTIM) GO TO 533
0166            INITIM=CURTIM
0167            IF (ICHECK.GE.2) IWRITE=1
0168            K=K+1
0169            GO TO 135
0170        533 WRITE (6,488) COUNT1
0171            WRITE (6,488) COUNT2
0172            WRITE (6,488) COUNT3
0173            WRITE (6,488) COUNT4
0174            WRITE (6,488) COUNT5
```

```
0175      488 FORMAT (/,1X,'COUNTS PER SECOND',//,(' ',20I6))
0176          DO 717 J=1,K
0177          M=FSTSEC+J-1
0178          WRITE (7,719) COUNT1(J),COUNT2(J),COUNT3(J),COUNT4(J),COUNT5(J),M
0179      719 FORMAT (6I6)
0180      717 CONTINUE
0181          STOP 1
0182          END
```

FORTRAN IV G LEVEL 21   TPREAD   DATE = 77270   13/20/20

```
0001              SUBROUTINE TPREAD
          C  READS RECORDS FROM WALLOPS FARADAY ROTATION DATA TAPES.
0002              INTEGER*2 ARRAY(2008)
0003              INTEGER*4 RECHRS,RECMIN
0004              COMMON ARRAY,TIMPRT,NUMREC,NUMHED,NUMCAL,RECHRS,RECMIN,RECSEC
          C  SKIP HEADER RECORDS
0005              DO 100 L=1,NUMHED
0006              READ (12,801,ERR=1000,END=2000) (ARRAY(M),M=1,10)
0007          801 FORMAT (10A2)
0008              NUMREC=NUMREC+1
0009              WRITE (11,807)
0010          807 FORMAT (1K,'HEADER RECORD READ')
0011          100 CONTINUE
          C  SKIP CALIBRATION RECORDS
0012              DO 110 L=1,NUMCAL
0013              READ (12,802,ERR=1000,END=2000) (ARRAY(M),M=1,1005)
0014          802 FORMAT (5(201A2))
0015              WRITE (11,808)
0016          808 FORMAT (1X,'CAL RECORD READ')
0017          110 NUMREC=NUMREC+1
0018              RETURN
0019              ENTRY DAREAD (IWRITE)
          C  READ DATA RECORD
0020              READ (12,803,ERR=1000,END=2000) ARRAY
0021          803 FORMAT (8(251A2))
0022              NUMREC=NUMREC+1
0023              WRITE (11,809) NUMREC
0024          809 FORMAT (1X,'DATA RECORD',I4,' READ')
0025              CALL GETIME
0026              IF (IWRITE.NE.1) RETURN
0027              WRITE (11,805) NUMREC
0028          805 FORMAT (//1X,'RECORD NUMBER: ',I4)
0029              WRITE (11,806) ARRAY
0030          806 FORMAT (/101(' ',2016/))
0031              RETURN
0032         1000 WRITE (11,1010)
0033         1010 FORMAT (1X,'*TPREAD*   TAPE ERROR')
0034              STOP 2
0035         2000 WRITE (11,2010)
0036         2010 FORMAT (1X,'*TPREAD*   END OF TAPE FILE')
0037              STOP 3
0038              END
```

FORTRAN IV G LEVEL 21   GETIME   DATE = 77270   13/20/20

```
0001          SUBROUTINE GETIME
0002          REAL MULT,MSECS
0003          COMMON 1,TIME,NUMREC,NUMHED,NUMCAL,RECHRS,RECMIN,RECSEC
0004          INTEGER*4 RECHRS,RECMIN,TIME
0005          INTEGER*2 I(2008),K(16)
0006          IWDNUM=2006
0007       20 ITIME=I(IWDNUM)
0008          IST=1
0009          IF(ITIME.GE.0) GO TO 30
0010          K(16)=1
0011          ITIME=ITIME+32768
0012          IST=2
0013       30 DO 50 M=IST,16
0014          N=17-M
0015          ITEST=2**(N-1)
0016          IF(ITIME.GE.ITEST) GO TO 70
0017          K(N)=0
0018          GO TO 50
0019       70 K(N)=1
0020          ITIME=ITIME-ITEST
0021       50 CONTINUE
0022          IF(ITIME.NE.0) WRITE(6,800)
0023      800 FORMAT (1X,'ERROR IN READING TIME WORD.  RESULT NOT ZERO')
0024          IF(IWDNUM-2007) 100,200,300
0025      100 MULT=0.0001
0026          MSECS=0.0
0027          DO 110 IDX=1,13,4
0028          ITMSEC=8*K(IDX+3)+4*K(IDX+2)+2*K(IDX+1)+K(IDX)
0029          MSECS=MSECS+(ITMSEC*MULT)
0030          MULT=MULT*10.
0031      110 CONTINUE
0032          IWDNUM=2007
0033          GO TO 20
0034      200 RECSEC=40*K(7)+20*K(6)+10*K(5)+8*K(4)+4*K(3)+2*K(2)+K(1)+MSECS
0035          RECMIN=40*K(15)+20*K(14)+10*K(13)+8*K(12)+4*K(11)+2*K(10)+K(9)
0036          IWDNUM-2008
0037          GO TO 20
0038      300 RECHRS=2-*K(6)+10*K(5)+8*K(4)+4*K(3)+2*K(2)+K(1)
0039          IF (TIME.GE.1) WRITE (11,805) RECHRS,RECMIN,RECSEC
0040      805 FORMAT ('+',28X,'TIME: ',I2,I2,':',F7.4)
0041          RETURN
0042          END


0001          SUBROUTINE UTIME (TIM,HRS,MINS,SECS)
0002          REAL*4MINS
0003          TI1=TIM/3600.
0004          HRS=AINT(TI1)
0005          REM1=AMOD(TIM,3600.)
0006          ATI2=REM1/60.
0007            S-AINT(ATI2)
```

```
0008          SECS=AMOD(REM1,60.)
0009          RETURN
0010          END
```

END
DATE

JUL 31, 1979